

# FINAL TECHNICAL REPORT

---

DE-FG07-00SF22172

**Design and Construction of a Prototype Advanced On-Line  
Fuel Burn-up Monitoring System for the Modular Pebble Bed  
Reactor**

March 30, 2004

**University of Cincinnati**



# PROJECT TITLE PAGE

**Project Title:** **Design and Construction of a Prototype Advanced On-Line Fuel Burn-up Monitoring System for the Modular Pebble Bed Reactor**

**Project Period:** August 1, 2000 – December 31, 2003

**Date of Report:** **March 30, 2004**

**Recipient:** University of Cincinnati  
2624 Clifton Avenue, Cincinnati, OH 45221

**Award Number:** DE-FG07-00SF22172

**Project Number:** 00-100

**Principal  
Investigator:** Dr. Bingjing Su  
University of Cincinnati

**Team Members:** Dr. Ayman Hawari  
North Carolina State University

**Dr. Ray Wood**  
**University of Cincinnati**

**Consultant:** Dr. Andrew C. Kadak  
Massachusetts Institute of Technology

## **DISCLAIMER**

Any opinions, findings, and conclusions or recommendations expressed in this report are those of the authors and do not necessarily reflect the views of the Department of Energy.

## EXECUTIVE SUMMARY

Modular Pebble Bed Reactor (MPBR) is a high temperature gas-cooled nuclear power reactor currently under study as a next generation reactor system. In addition to its inherently safe design, a unique feature of this reactor is its multi-pass fuel circulation in which the fuel pebbles are randomly loaded and continuously cycled through the core until they reach their prescribed End-of-Life burn-up limit. Unlike the situation with a conventional light water reactor, depending solely on computational methods to perform in-core fuel management for MPBR will be highly inaccurate. An on-line measurement system is needed to accurately assess whether a given pebble has reached its End-of-Life burn-up limit and thereby provide an on-line, automated go/no-go decision on fuel disposition on a pebble-by-pebble basis.

This project investigated approaches to analyzing fuel pebbles in real time using gamma spectroscopy and possibly using passive neutron counting of spontaneous fission neutrons to provide the speed, accuracy, and burn-up range required for burnup determination of MPBR. It involved all phases necessary to develop and construct a burn-up monitor, including a review of the design requirements of the system, identification of detection methodologies, modeling and development of potential designs, and finally, the construction and testing of an operational detector system. Based upon the research work performed in this project, the following conclusions are made.

In terms of using gamma spectrometry, two possible approaches were identified for burnup assay. The first approach is based on the measurement of the absolute activity of Cs-137. However, due to spectral interference and the need for absolute calibration of the spectrometer, the uncertainty in burnup determination using this approach was found to range from  $\sim \pm 40\%$  at beginning of life to  $\sim \pm 10\%$  at the discharge burnup. An alternative approach is to use a relative burnup indicator. In this case, a self-calibration method was developed to obtain the spectrometer's relative efficiency curve based upon gamma lines emitted from  $^{140}\text{La}$ . It was found that the ratio of  $^{239}\text{Np}/^{132}\text{I}$  can be used in burnup measurement with an uncertainty of  $\sim \pm 3\%$  throughout the pebble's lifetime. In addition, by doping the fuel with  $^{60}\text{Co}$ , the use of the  $^{60}\text{Co}/^{134}\text{Cs}$  and  $^{239}\text{Np}/^{132}\text{I}$  ratios can simultaneously yield the enrichment and burnup of each pebble. A functional gamma-ray spectrometry measurement system was constructed and tested with light water reactor fuels. Experimental results were observed to be consistent with the predictions.

On using the passive neutron counting method for the on-line burnup measurement, it was found that neutron emission rate of an irradiated pebble is sensitive to its burnup history and the spectral-averaged cross sections used in the depletion calculations; thus a large uncertainty exists in the correlation between neutron emission and burnup. At low burnup levels, the uncertainty in the neutron emission/burnup correlation is too high and neutron emission rate is too low so that it is impossible to determine a pebble's burnup by on-line neutron counting. At high burnup levels, due to the decreasing of the uncertainty in neutron emission rate and the super-linear feature of the correlation, the uncertainty in burnup determination was found to be  $\sim 7\%$  at the discharge burnup, which is acceptable for determining whether a pebble should be discharged or not. In terms of neutron detection, because an irradiated pebble is a weak neutron source and a much stronger gamma source, neutron detector system should have high neutron detection efficiency and strong gamma discrimination capability. Of all the commonly used neutron detectors, the He-3 and  $\text{BF}_3$  detector systems were found to be able to satisfy the requirement on detection efficiency; but their gamma discrimination capability is only marginal for this on-line application. Even with thick gamma shielding, these two types of detectors shall deteriorate in performance after a certain period of time of operation. Thus, two or more

detector systems must be used alternatively for continuous measurement. On the other hand, fission chambers were found that they can effectively discriminate gamma interference for this on-line application even without using gamma shield. However, detection efficiency of fission chambers is low; so a multi-fission-chamber system (using at least 12 commercially available fission chambers) must be constructed in order to achieve the required detection efficiency. Overall, passive neutron counting could be used to provide an on-line, go/no-go decision on fuel disposition on a pebble-by-pebble basis for MPBR, if the detection system is well designed.

## TABLE OF CONTENTS

<b>Project Title Page</b>	<b>ii</b>
<b>Disclaimer</b>	<b>iii</b>
<b>Executive Summary</b>	<b>iv</b>
<b>1. Introduction</b>	<b>1</b>
<b>2. Project Objective and Work Scope</b>	<b>2</b>
<b>3. Burnup Measurement by Gamma-Ray Spectrometry</b>	<b>5</b>
<b>4. Burnup Measurement by Neutron Counting</b>	<b>24</b>
<b>5. Conclusion</b>	<b>37</b>
<b>6. Reference</b>	<b>38</b>
<b>Appendix – Publication Developed under This Project</b>	<b>39</b>

## 1. INTRODUCTION

The Modular Pebble Bed Reactor (MPBR) is a high temperature gas-cooled nuclear power reactor that is currently under study as a next generation reactor system. Nominally the MPBR is designed to have a core power of 250 to 300 MW-thermal. The fuel elements for this reactor are spherical pebbles that are composed of an outer graphite shell (0.5 cm thick) surrounding an inner fuel zone (2.5 cm radius). The fuel zone has a graphite matrix in which approximately 11,000 silicon carbide (SiC) coated fuel micro-spheres (of 0.9 mm diameter) are embedded. The SiC coating assures that no fission products are released from the micro-spheres. Depending on the details of the core design, each pebble contains a total of 7 to 9 gram of UO<sub>2</sub> enriched to approximately 8% in U-235. Present MPBR designs describe cores that contain a total of 330,000 to 360,000 fuel pebbles [1-3]. In addition to its inherently safe design, a unique feature of this reactor is its multi-pass fuel circulation in which the fuel pebbles are randomly loaded and continuously cycled through the core until they reach their prescribed End-of-Life burn-up limit (80,000 MWD/MTU). On average, a pebble will cycle the core ten times before being discharged. Obviously, when a pebble comes out of the reactor barrel its burnup should be known in order to determine whether it should be discharged or not. However, due to the multi-pass and random circulation of a pebble through the core, its neutron flux exposure history is unknown. Therefore, unlike the situation with a conventional light water reactor (LWR), depending solely on computational methods to perform in-core fuel management for MPBR will be highly inaccurate; and an on-line measurement system is needed to accurately assess whether a given pebble has reached its End-of-Life burn-up limit and thereby provide an on-line, automated go/no-go decision on fuel disposition on a pebble-by-pebble basis. This logic is shown in Fig. 1.1. The goal of this DOE-NERI project is to conceptually design, construct and test an advanced on-line fuel burn-up monitoring system for MPBR.

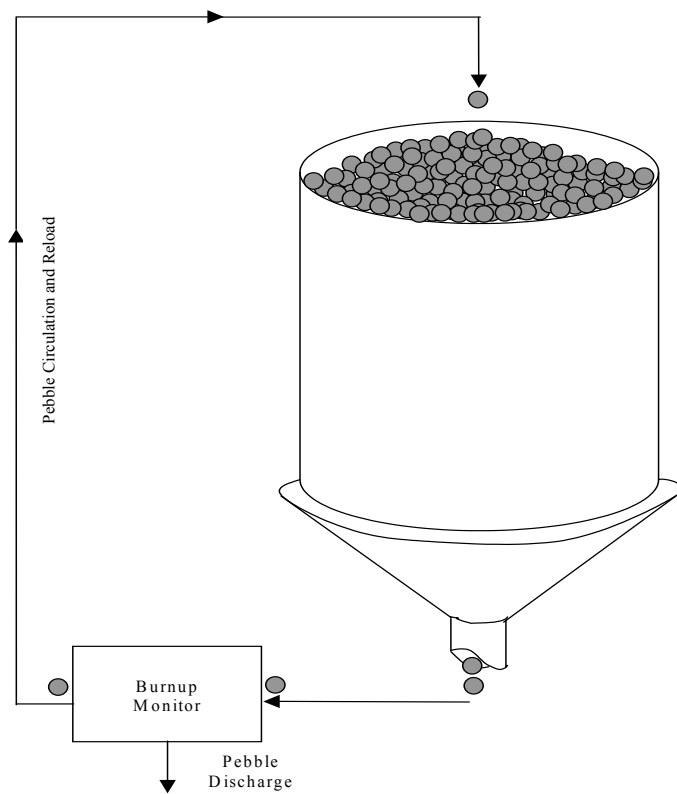


Fig. 1.1. A simplified schematic of the fuel circulation in a MPBR.

## 2. PROJECT OBJECTIVE AND WORK SCOPE

This project investigates approaches to analyzing pebble bed fuel in real time using gamma spectroscopy and possibly using passive neutron counting of spontaneous fission neutrons to provide the speed, accuracy, and burn-up range required for the determination of burnup for MPBR. It involves all phases necessary to develop and construct a burn-up monitor, including a review of the design requirements of the system, identification of methodologies that would satisfy the design requirements, modeling and development of potential designs, and finally, the construction and testing of an operational detector system. Specifically, this project has five tasks:

### **Task 1 – Identification of System Requirements**

The objective of task 1 is to identify the design requirements for an on-line burnup monitoring system to be used with the MPBR design. This task involves collecting the most recent design parameters from the MPBR design effort underway at MIT, INEEL and South African ESKOM. The collected results are used as the design basis for determining the availability and physical requirements of the burnup monitor, including pebble size, pebble configuration, pebble throughput rates, burnup ranges of interest, core design, and any special physical requirements for handling the fuel pebbles, such as cool down time for pebbles prior to measurement. The product of this task is a set of requirements for the burnup monitor to ensure that the components are operating within their allowable ranges and duty cycles.

### **Task 2 – Depletion Modeling**

The fundamental prerequisite for the monitoring system design is to identify correlations between a measurable quantity of radiation and fuel burnup. These correlations must be well defined and valid over the burnup range of interest. For a system using gamma or neutron measurement techniques, this requires identifying potential isotopes or groups of isotopes that provide a radiation source varying in a manner that can be correlated to the fluence experienced by the fuel. Calculation of isotopic quantities as a function of burnup is to be performed using the computer code ORIGEN2. The ORIGEN code family is a set of codes developed by Oak Ridge National Laboratory for calculating the depletion of fuel isotopes and the build-up of fission product and transuranic isotopes in fuel undergoing irradiation. As input, the ORIGEN codes require information on the fuel material and enrichment, specific power densities within the reactor, and libraries of cross section and yield data for various energy spectrums. Unfortunately, ORIGEN2 does not have cross section and yield libraries that are directly applicable to pebble bed reactor (PBR) design. To eliminate the uncertainty in the burnup/radiation correlation caused by the lack of appropriate libraries, MPBR-specific cross section libraries should be constructed based on calculated neutron energy spectrum, before various burnup depletion calculations for the MPBR fuel pebbles are performed. Because the pebbles are moving randomly through a reactor where the spatial variation of flux is high, irradiation fluence level experienced by a fuel pebble per trip through the reactor is expected to fluctuate and its effect on the depletion calculations is to be quantified. The results from this task provide the activities and concentrations of fission products and transuranic isotopes as a function of fuel burnup under different conditions.

### **Task 3 – Radiation/Burnup Analysis (Finding Burnup Indicators)**

The objective of task 3 is to analyze radiation versus burnup data and identify candidate correlations that can

relate some type of radiation emitted from a fuel pebble and its burnup. Strictly speaking, there is no one-to-one relationship between radiation emission and burnup, because radiation emission not only depends upon the accumulative burnup but also depends upon the details of burnup history (i.e., how that burnup is achieved). Due to the random, multi-pass circulation of a pebble through the reactor core, the burnup history of an individual pebble can not be known. The goal is to identify some selected signatures (types, amounts and spectra) of radiation emitted from a fuel pebble that are strong functions of the accumulative burnup but are only weak functions of the burnup history so that they can be used as burnup indicators. Ideal correlations should have strong, clearly measurable signals with minimal interference from non-correlated sources, and can be described by functions that are well behaved over the important burnup ranges. In addition, a good correlation should exhibit large changes in measurable radiation for small changes in burnup because the ratio of change in measurable signal change to change in fuel burnup determines the theoretical accuracy of the estimation allowed by the correlation. The presence of interfering signals in the measurement from isotopes present in the fuel that are not part of the correlation of interest can increase the uncertainty in the correlation. Interferences in gamma spectrometry typically include gamma rays emitted by fission products with gamma energies close to those of interest. In addition, the extremely high activity levels associated with irradiated fuel tend to make gamma spectra so complex that resolving individual peaks becomes more difficult. Interferences for neutron counting systems generally include sources such as delayed neutrons and neutrons produced by  $(\alpha, n)$  reactions, either of which may interfere with the spontaneous fission neutrons of interest. Uncertainty in the identified correlations is estimated by considering depletion data for different irradiation histories. The outputs of this task are candidate correlations of fuel pebble burnup to emitted radiation, along with an estimate of the uncertainty of the correlations.

#### **Task 4: Detection Simulation and Design of the Detector System**

Once the candidate radiation/burnup correlations are identified, investigation focuses on evaluating whether the selected radiation signatures (or burnup indicators) can be measured accurately for the on-line measurement. The requirement of on-line application poses additional difficulties in measurement, such as strong radiation source/noise and short measurement time. This task involves using the isotopic concentration data and MCNP simulation to model radiation emission from an irradiated fuel pebble and develop signal-to-source response functions for various types of detectors and identify the best detector system for use in the burnup monitor. Task 4 consists of 3 subtasks:

*Subtask 4.1:* Identify potential detectors for neutron counting and gamma ray spectrometry. A variety of detector types are to be evaluated for their effectiveness in the burnup monitoring system. The evaluation criteria include the system requirements as determined earlier, as well as detector efficiency and effectiveness in regions of interest as determined from the correlations identified in task 3. Detector types and arrangements that meet the requirements are considered as candidate detector systems. Neutron detectors to be considered include, but are not limited to, fission chambers,  $BF_3$  tubes, boron-lined tubes, and  $He-3$  tubes. Gamma detectors to be considered are solid-state detectors such as high purity germanium (HPGe) detector.

*Subtask 4.2:* Detector selection and optimization. After one or more burnup correlations and candidate detector types have been identified, combinations of detector systems are modeled using MCNP simulation for each detector type and geometry. For each detector system, measurable quantities, such as count rates and peak areas, are related to burnup. Overall uncertainty in the burnup measurement is estimated by combining uncertainties in the expected isotopic activities and concentrations, calculated detector efficiencies, and

Poisson counting statistics. In addition, all other issues related with the on-line measurement are to be studied.

*Subtask 4.3:* Conceptual system design. During this subtask a burnup monitor system design is finalized, which includes the detector, real-time data acquisition system and associated internal logic that calculates fuel pebble burnup.

### **Task 5 – Construction of a Prototype Monitor System and Demonstration**

Based upon the conceptual system design, a prototype burnup monitor system is constructed during the final phase of the project. Following construction, the system is tested experimentally to benchmark against the computer simulations in order to verify the correlations and all the issues related with the measurement. Due to the unavailability of real irradiated fuel pebbles, benchmarking is to be accomplished through gamma ray spectrometry using LWR fuels that have been irradiated in a research reactor. Such experiments will demonstrate the ability of the detector system to handle the complex spectra from burned fuel.

All of these proposed tasks were completed successfully. The technical details on these tasks are reported in the following two sections. Section 3 summarizes the work on burnup measurement by gamma-ray spectrometry and Section 4 summarizes the work on burnup measurement by neutron counting.

### 3. BURNUP MEASUREMENT BY GAMMA-RAY SPECTROMETRY

The gamma-ray spectrum of a fuel pebble is expected to be very complicated, because hundreds of radioactive isotopes are produced during the irradiation of the pebble within the reactor. Among all the gamma-ray spectroscopy detectors, HPGe detectors have the best energy resolution. Therefore, a burn-up monitoring system using an HPGe detector is proposed and is depicted in Figure 3.1. A computational method using ORIGEN2, MCNP and SYNTH is employed to simulate the gamma-ray spectrum for a fuel pebble at different burn-up steps.

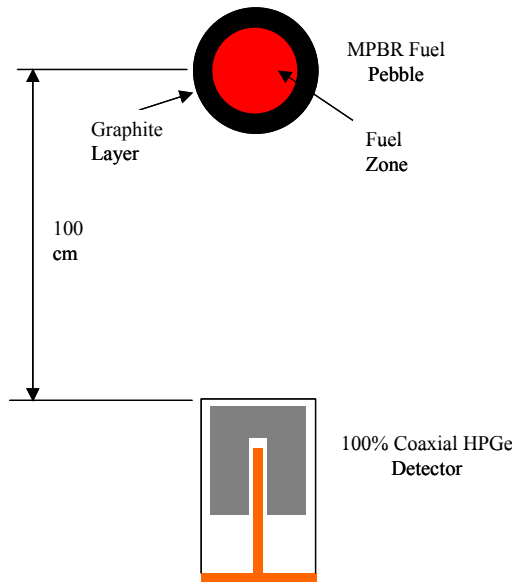


Figure 3.1 Proposed Gamma-ray Burnup Monitoring System

#### 3.1 ORIGEN2 Fuel Depletion Calculation

To simulate a gamma-ray spectrum of a fuel pebble, reliable fuel isotopic inventory needs to be determined at different burnup steps to construct the gamma source term. The ORIGEN2 code is used to perform the fuel depletion calculation to simulate the in core process of a fuel pebble. However, there is no established cross section library for High Temperature Gas Reactors, either for ORIGEN2 or for other fuel depletion codes. In this work, an effort has been made to generate reliable cross sections for Pebble Bed Reactor.

##### 3.1.1 Cross Section Library Generation for ORIGEN2

ORIGEN2 uses one-group averaged cross sections, which are provided by an external program specifically targeting a particular system it is simulating, to perform the fuel cycle burnup calculation. The one-group averaged cross section is calculated by

$$\bar{\sigma} = \frac{\int_0^{\infty} \sigma(E) \cdot \Phi(E) \cdot dE}{\int_0^{\infty} \Phi(E) \cdot dE} \quad (3.1)$$

where  $\Phi(E)$  is the neutron energy spectrum calculated for a certain type of reactor by neutron transport codes. There are many factors that affect the neutron energy spectrum in the fuel, such as system operation temperature, fuel geometric structure, and fuel isotopic compositions (burnup). A special MCNP model is developed for the PBR to investigate its neutron energy spectrum.

### 3.1.1.1 Heterogeneous Core Modeling with Microsphere Fuel Kernels

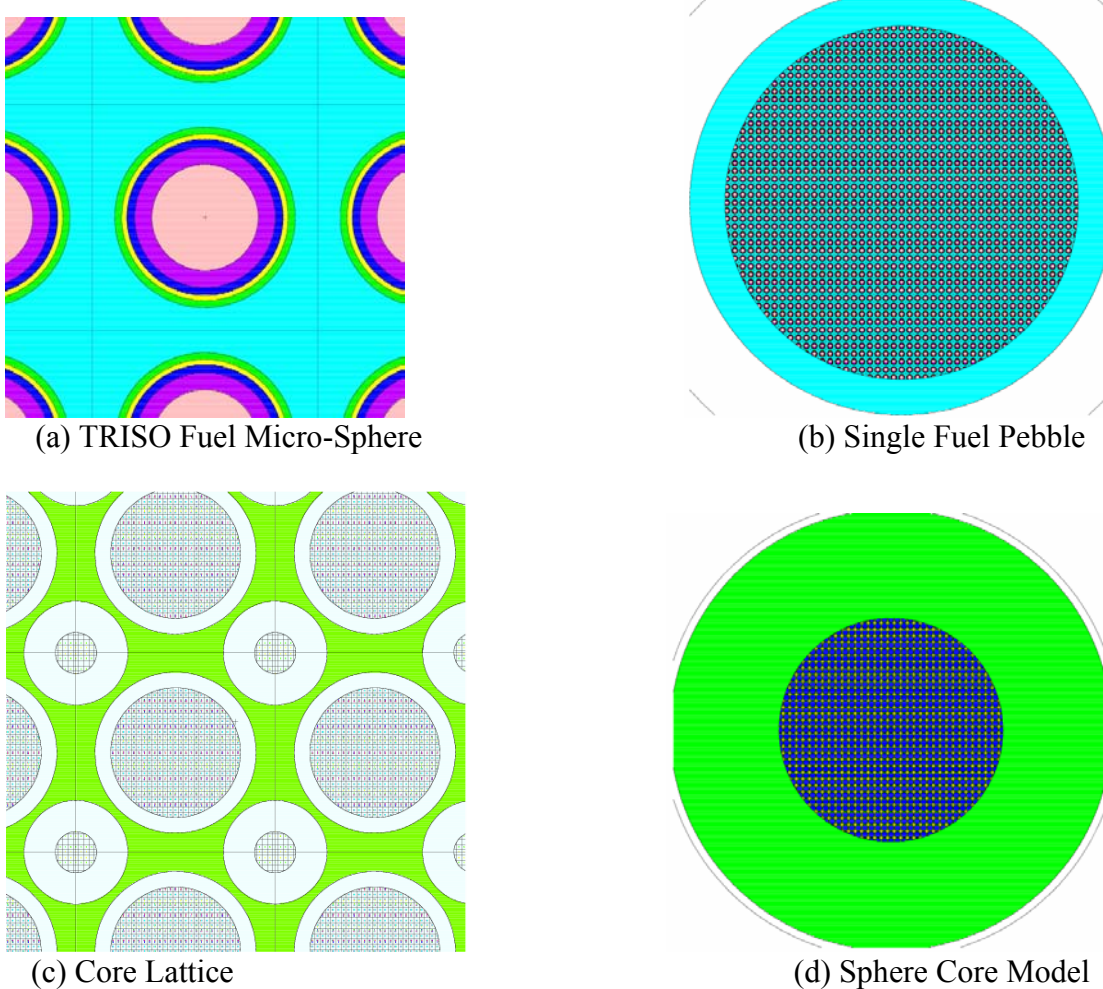


Figure 3.2 Configuration of the double-heterogeneous PBR Model

A spherical double heterogeneous MCNP5 model consisting of a single fuel sphere in the center, surrounded by a 1 m fuel driver zone (piled up with fuel spheres) and a 1 m graphite reflector is constructed for the PBR. The first level heterogeneity is implemented at fuel micro-sphere lattice level, in which a TRISO fuel model has a 530  $\mu\text{m}$ -diameter  $\text{UO}_2$  kernel surrounded first by one buffer layer of low density carbon and then two pyro-carbon layers with one layer of  $\text{SiC}$  in between. This lattice structure is then filled into a 5 cm-diameter fuel zone surrounded by a 0.5 cm thick graphite shell to model a single fuel pebble. There are about 11,000 fuel micro-sphere kernels contained in one fuel pebble. The second level of heterogeneity is implemented at the reactor core lattice level. The basic unit of a core lattice consists of a body-center-cubic cell. A single cell

contains a complete fuel pebble in the center and eight one-eighth pebbles, one in each of the corners of the cell. This double-heterogeneous geometric configuration of the PBR model is shown in Figure 3.2.

Using this double-heterogeneous MCNP model, two types of criticality KCODE calculations were performed for the fresh fuel loaded core. One was applied with S ( $\alpha$ ,  $\beta$ ) thermal treatment at 1200 Kelvin, which is the operation temperature of PBR, while the other used the MCNP default free gas thermal treatment model at 293.6 K. In both calculations, neutron flux in the fuel kernels at the center fuel pebble volume was tallied within 501 energy bins. Based on these neutron spectra, two sets of one-group spectrum-averaged cross sections of fresh fuel pebbles were generated for selected nuclides. In addition, the neutron spectrum from MIT-INEEL work was also used to produce another set of cross section data as a reference. All these data are listed in Table 3.1 to compare with the cross section values in the ORIGEN2 libraries and the PBR data published by the South Africa company, ESKOM. As shown in the table, the cross section data generated at the low temperature are similar to the MIT-INEEL data while the cross section data generated at 1200 K are close to the ESKOM data. The reason for such difference can be explained by considering the energy spectra and energy-dependent cross section structures.

Table 3.1 Comparison of one-group averaged cross sections for fresh fuel pebbles

Nuclide	ORIGEN CANDU	ORIGEN PWR	ORIGEN BWR	MIT-INEEL	ESKOM	This Work 293.6 K	This Work 1200 K
Cs-137 (n, $\gamma$ )	0.068	0.026	0.026	0.045	N/A	0.045	0.036
Cs-133 (n, $\gamma$ )	22.6	10.7	10.9	20.3	N/A	18.6	16.0
Cs-134 (n, $\gamma$ )	77.2	16.8	16.8	31.4	N/A	34.7	27.0
Co-59 (n, $\gamma$ )	21.5	2.2	2.3	10.9	N/A	11.3	8.93
U-235 (n, $\gamma$ )	24.5	10.5	11.2	25	22.5	26.6	20.7
U-238 (n, $\gamma$ )	1.06	0.90	0.92	6.69	3.25	4.01	3.46
Pu-239 (n, $\gamma$ )	115	59	63	108	264	108	249
Pu-241 (n, $\gamma$ )	100.2	38.7	41.5	91.5	135.8	97.7	123
U-235 (n,f)	134	47	50	126	107	138	99.3
U-238 (n,f)	0.056	0.100	0.081	0.022	0.025	0.036	0.028
Pu-239 (n,f)	240	106	114	224	428	232	406
Pu-241 (n, f)	295	118.1	126.3	265	361.6	282	330

### 3.1.1.2 Burnup Dependent Cross Sections

MCNP/ORIGEN2/monteburns code system was used to investigate the effect of fuel isotopic compositions on PBR neutron spectrum, and thus to develop burnup dependent cross section data for PBR. Monteburns is a fully automated tool that is designed to link MCNP and ORIGEN2 to perform a Monte Carlo burnup calculation. Burnup-dependent neutron energy spectrum for PBR is significantly different from that of a traditional PWR: for the PWR, the neutron spectrum within the fuel assembly is dominated by the burnup of the fuel assembly itself; while for the PBR it is mostly determined by the burnup of the surrounding fuel spheres, with the burnup of the fuel sphere itself only playing a secondary role. This is caused by the fact that PBR has a much greater neutron mean free path than PWR, which allows neutrons to escape from the fuel element where they are originated, and be thermalized and absorbed in a fuel sphere relatively far from where they are produced.

For the MCNP/ORIGEN2/monteburns coupled simulations, the power density is assumed to be 5.25 MW/m<sup>3</sup>, which is similar to the power density of ESKOM design, and the core is assumed to be burnt up to 100,000 MWD/MTU in 40 equal outer burn steps in monteburns. For each outer burn step, MCNP calculates one-group microscopic cross sections and fluxes that are used by ORIGEN2 in depletion calculations. Then monteburns extracts the information on isotopic compositions from the ORIGEN2 output file, and passes them back to MCNP to update the material compositions for the MCNP input file for the next burnup step. In this way, the one-group spectral averaged cross sections for a total of 37 radionuclides were generated for fresh fuel core, at 50,000MWD/MTU and 10,000MWD/MTU burnup levels. Some data are listed in Table 3.2.

Table 3.2 Burnup Dependent Cross Sections (at 1200 K) for PBR

Nuclide	Fresh fuel core	50,000 MWD/MTU	100,000 GWD/MTU
Cs-137(n,γ)	0.036	0.036	0.038
Cs-133(n,γ)	16.0	15.9	15.8
Cs-134(n,γ)	27.0	26.3	29.9
Co-59(n,γ)	8.93	8.74	9.53
U-235(n,γ)	20.7	20.2	22.7
U-238(n,γ)	3.46	3.57	3.40
Pu-239(n,γ)	249	235	271
Pu-241(n,γ)	123	118	136
U-235(n,f)	99.3	96.4	111
U-238(n,f)	0.028	0.030	0.027
Pu-239(n,f)	406	385	444
Pu-241(n,f)	330	316	366

### 3.1.2 ORIGEN2 Fuel Cycle Simulation

For pebble bed reactors, fuel pebbles are continuously circulating through the reactor core until they reach the proposed burnup limit (~ 80,000 MWD/MTU). When pebble flows from the top of the core down to the bottom, it is traveling mostly in the axial direction, with little moving in the radial direction. In addition, it is expected that pebbles loaded at the center of the core are traveling at a faster speed than those loaded at the peripheral region of the core. Due to the spatial distribution of neutron flux within the PBR core, a pebble is exposing to higher neutron flux level when it is traveling in the center zone of the core than when it is passing through the peripheral zones. Besides, the average burnup of fuel region surrounding the fuel pebble has an effect on its neutron energy spectrum, hence different burnup-dependent cross sections should be used to account for this variation. Based on the above analysis, nine ORIGEN2 calculations have been run to consider different fuel burnup histories. For each of the three sets of burnup-dependent cross sections, three burnup rates were used to perform a 10-pass fuel cycle simulation to reach 100,000 MWD/MTU, with the assumption of 48-hour cooling time per pass.

### 3.2 MCNP/SYNTH Gamma-ray Spectrum Simulation

The results of ORIGEN2 depletion calculation provides only isotopic compositions and gamma source terms in a very coarse energy structure of 18-group photon bins, which is not good enough for an accurate gamma-ray spectrometry analysis. Also, energy strangling should be considered in MCNP simulations in order to

obtain a realistic gamma-ray spectrum.

### 3.2.1 Gamma-ray Source Term Construction

ORIGEN2 depletion calculations produce a total of 344 radionuclides of non-zero activity. A program called SYNTH was utilized to establish the gamma ray source term based upon these radionuclides. SYNTH is a synthetic gamma-ray spectrometry software developed by Pacific Northwest National Laboratory. It contains three comprehensive nuclear databases for radionuclides: half-life, gamma line energy, and branching ratio. SYNTH can generate most gamma lines emitted from the 344 radionuclides resulted from the ORIGEN2 depletion simulations and results show that a total of 11,840 gamma lines are picked up for the 344 radionuclides produced within the fuel pebble.

To construct the source term, the source input energy bin is refined as 0.5 keV/channel, extending from 0 MeV to 10 MeV. The intensity probability distribution for each bin is calculated as

$$P_{E_k} = \frac{\sum_{i=1}^N A_i \Gamma_{i,E_k}}{\sum_{E_k=E_0}^{E_{\max}} \sum_{i=1}^N A_i \Gamma_{i,E_k}} \quad (3.2)$$

where  $E_k$  is the k-th energy bin;  $N$  is the total number of radionuclides contributing to the gamma source;  $A_i$  is the activity of i-th radionuclide;  $\Gamma_{i,E_k}$  is the branching ratio for i-th radionuclide emitting a gamma-ray at energy  $E_k$ . A program was written in C++ to input this source probability distribution into the MCNP models.

### 3.2.2 Full Width Half Maximum (FWHM) vs. Energy

The detector response function can be simulated by performing a photon-electron transport calculation using the F8 pulse height tally in MCNP. The pulse height tally provides the energy distribution of pulses created in a cell that models a physical detector (i.e., the active volume in a HPGe detector). However, this tally does not account for the statistical variation in the number of charged carriers produced by the interactions of gamma rays in the detector. Therefore, the full energy peak in the spectrum of a monoenergetic source is a perfect delta-function, which is impossible for a real detector system. A realistic detector system has finite energy resolution so its response to a monoenergetic source in fact is a Gaussian-like peak. The treatment of Gaussian Energy Broadening (GEB) was applied to simulate this effect. Specifically, SYNTH was used to find that the FWHM characteristic of the model detector system is given by

$$\text{FWHM} = 1.92112 \times 10^{-6} + 1.64456 \times 10^{-3} \cdot \sqrt{E - 3.04804 \times 10^{-5} E^2} \quad (3.3)$$

This relationship was used to broaden the full energy peaks in the MCNP model.

### 3.2.3 Simulated Gamma-ray Spectra

With the gamma source term constructed and a realistic FWHM vs. energy relationship developed, the gamma-ray spectrum were simulated for the MCNP model of the prototype detection system at different burnup steps, namely, 20,000 MWD/MTU, 50,000 MWD/MTU, and 80,000 MWD/MTU. Due to the huge difference in gamma counts, variance reduction techniques had to be used in the MCNP simulations. Shown in Figure 3.3 is the gamma-ray spectrum at 20,000 MWD/MTU. The simulated spectra are normalized to the

counts in a multi-channel analyzer assuming a counting time period of 30 seconds. Based on these spectra, a series detailed gamma-ray spectroscopy analyses (peak interference check, Minimum Detectability check, error analysis) were performed to find burnup indicators that can be used for the on-line fuel burnup measurement by gamma-ray spectrometry.

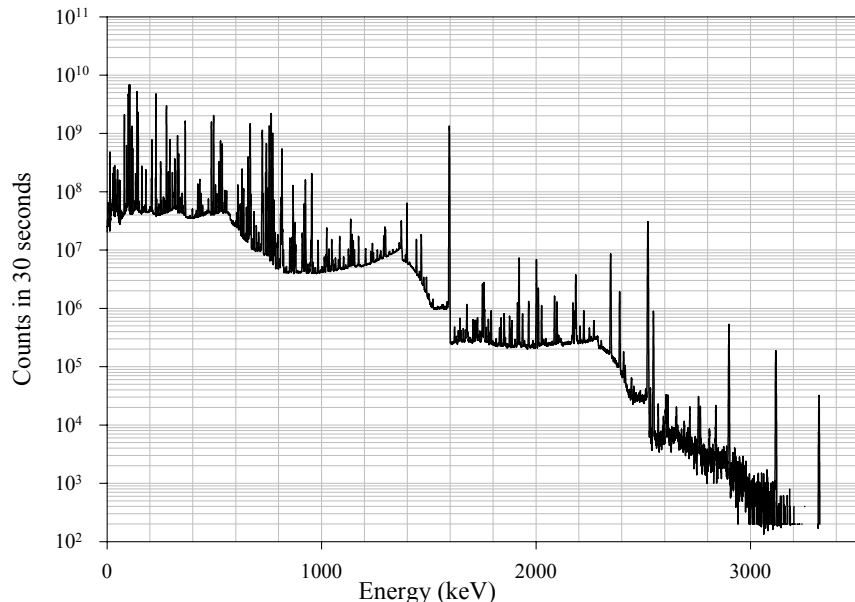


Figure 3.3 Simulated Gamma-ray Spectrum for PBR fuel at 20,000 MWD/MTU

### 3.3 Evaluation of Absolute Activity Burnup Indicators

Fuel burnup is directly related to the fission reactions that take place in a given fuel element. Ideally, burnup can be assessed by measuring the amount of fissile material left in the fuel if the initial fuel enrichment is known. However, passive nondestructive methods are not capable of yielding that information directly due to the existence of very strong radiation sources in irradiated fuel that will overwhelm direct signatures of the fissile material. Therefore, passive burnup measurements have to be performed indirectly using the spontaneous emission of gamma and neutron radiation by the fission products and heavy actinides that result upon irradiation of the fuel. To identify all the possible burnup indicators, the radionuclides produced by ORIGEN2.1 were scrutinized based on some criteria developed below.

#### 3.3.1 Absolute Activity Burnup Indicator Selection Criteria

As stated earlier, the ORIGEN2.1 simulations assumes a PBR power of 265 MW-thermal, and UO<sub>2</sub> fuel that is enriched to 8% in U-235. The fuel is assumed to go through several periods of irradiation and cooling that simulate the circulation of the pebbles in and out of the core during a pebble's irradiation cycle. As a result, 344 non-zero activity radionuclides were produced that can be potentially used in passive assay of the fuel. However, the choice of a burnup indicator can be facilitated by observing three criteria:

- 1) For PBR, a fuel pebble may have a different travel path every time it is circulated through the core. It becomes clear that the ideal indicator should provide the required burnup information independent of the variations in the pebble's exposure history as it passes through the core. Two factors contribute

to this variation, one is the total neutron flux level the pebble is experiencing while it is passing different zones of the core; the other is the average burnup of fuel pebbles surrounding it in these zones, which affects the neutron spectrum and the one-group spectrum-averaged cross sections. Failure to fulfill this criterion will result in large uncertainties in the measurement of fuel burnup, which may lead either to operating with un-optimized fuel cycles, or to breaching the fuel operating safety limits and increasing the probability of fuel failure.

- 2) The indicator should have a monotonic increase or decrease relationship between activity and burnup in order to give a unique correlation that can be used to determine a certain burnup level. Also, the difference of activities between different burnup steps should be prominent (greater than the measurement uncertainty) to distinguish one burnup step from another.
- 3) The indicator should emit gamma rays that are detectable within the counting period of interest for on-line monitoring. In gamma-ray spectrometry, this criterion can be quantified using the minimum detectable activity (MDA) concept.

Consequently, many of the radionuclides that are produced in the depletion can be excluded from use as burnup indicators. To apply those criteria to find potential burnup indicators, a search program called AbsIsoSearch was written in C++ to perform data mining on the ORIGEN2.1 outputs.

### 3.3.2 Power (Burnup) History Variation Search

In this search, all 344 non-zero activity radionuclides produced by fuel depletion were examined one by one. For each radionuclide, the burnup steps are divided into 8 steps from 10,000 MWD/MTU to 80,000 MWD/MTU, and there are nine sets of activity vs. burnup data accounting for three different neutron energy spectra at three different total neutron flux levels. During the search process, the power history variation of a radionuclide was examined by looking at the differences among those nine activities corresponding to each burnup step. The criterion used here is that the maximum difference should be less than 15%. Also, the differences between a certain burnup step to its previous and next burnup steps are set to be greater than 5% to guarantee the radionuclide's activity can be used to distinguish one burnup step from another. A total of 21 gamma-emitters survived these tests.

### 3.3.3 Minimum Detectability Activity Check

For the 21 gamma-emitters to be useful as burnup indicators, the gamma rays have to be detectable on the background of the gamma-ray spectrum of the fuel pebble. The Minimum Detectable Activity (MDA) of a gamma line is calculated by

$$N_D = 3.29 \sqrt{N_B \left(1 + \frac{n}{2m}\right)} + 2.706 \quad (3.4)$$

$$MDA = \frac{N_D}{f\varepsilon T} \quad (3.5)$$

where  $N_B$  is the background counts;  $N_D$  is the minimum value of net source counts;  $n$  is the peak channel number;  $m$  is the background channel number;  $\varepsilon$  is the absolute detection efficiency;  $f$  is the gamma-ray yield per disintegration; and  $T$  is the counting time, which is 30 seconds.

Based up the simulated spectrum, MDA was calculated for the 21 gamma-emitters at a single pass burnup level (10,000 MWD/MTU). Results show that there are only 4 radionuclides whose activities greater than MDA and they are listed in Table 3.3. As shown, gamma peaks of Eu-154, Eu-155, and Kr-85 have an activity only barely greater than the MDA so they would be difficult to be identified from the spectrum. However, Cs-137 has an activity almost five orders of magnitude greater than the MDA; thus it is a good candidate as a burnup indicator.

Table 3.3 Four Gamma Emitters Passed the MDA Check

Radionuclides	Half-life (years)	Single Pass Activity (Ci/pebble)	MDA (Energy) (Ci/Pebble)
Cs-137/Ba-137M	30.02	0.210	0.00013 (661.7)
Eu-154	8.81	0.000653	0.00049 (1005)
			0.00035 (1275)
Eu-155	4.96	0.00425	0.00999 (87)
			0.00957 (105)
Kr-85	10.73	0.025	0.0431 (513)

### 3.3.4 Using Cs-137 as a Burnup Indicator

To further investigate the feasibility of using Cs-137 as a burnup indicator, the activities of Cs-137 within a pebble at different power levels and through different fuel zones were analyzed in detail. The error bounds for the burnup vs. activity correlation for Cs-137 is plotted in Figure 3.4, which shows that the low bound and high bound curves are very close so the correlation is not sensitive to burnup history. This is because Cs-137 has a very long half life (compared to the total in core time of 3 years) and a small neutron absorption cross section, so the amount of Cs-137 in the fuel is almost linearly proportional to burnup. In addition, the fission yield of Cs-137 is almost the same for both U-235 and Pu-239, which minimizes the effect of yield variation with fissile material on the burnup vs. activity correlation.

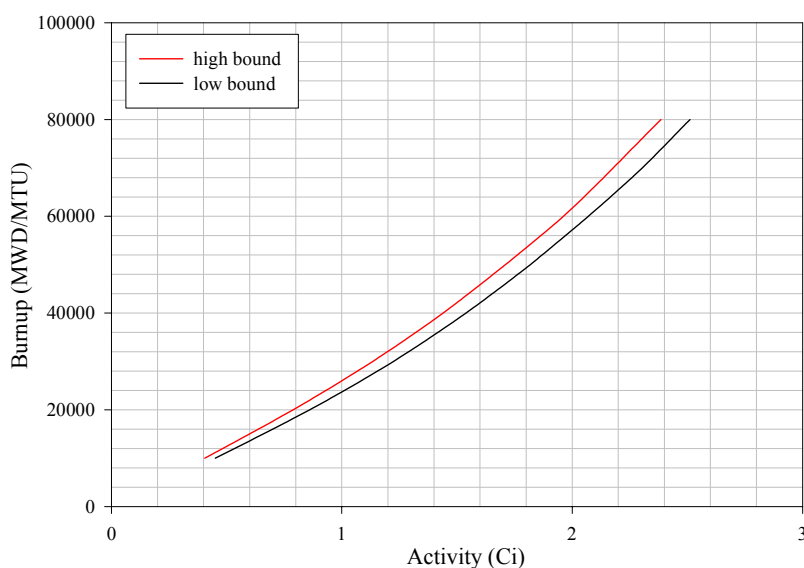


Figure 3.4 Burnup vs. Cs-137 Activity

### 3.3.4.1 Interference Check for the Gamma Line of Cs-137

Cs-137 has one major gamma peak (with branching ratio 0.85) at 661.7 keV. However, it was found that few strong gamma lines are emitted by other radionuclides around 661.7 keV, as shown in Table 3.4, which indicates that Cs-137 661.7 keV peak is interfered by Nb-97, I-132, and Ce-143 peaks. The detailed gamma-ray spectrum was analyzed by GammaVision, a widely used gamma-ray spectroscopy analysis software. Figure 3.5 presents the de-convoluted multiple-peak region of the spectrum at different burnup steps. As shown, the Cs-137 peak grows with burnup so it has less interference at higher burnup steps.

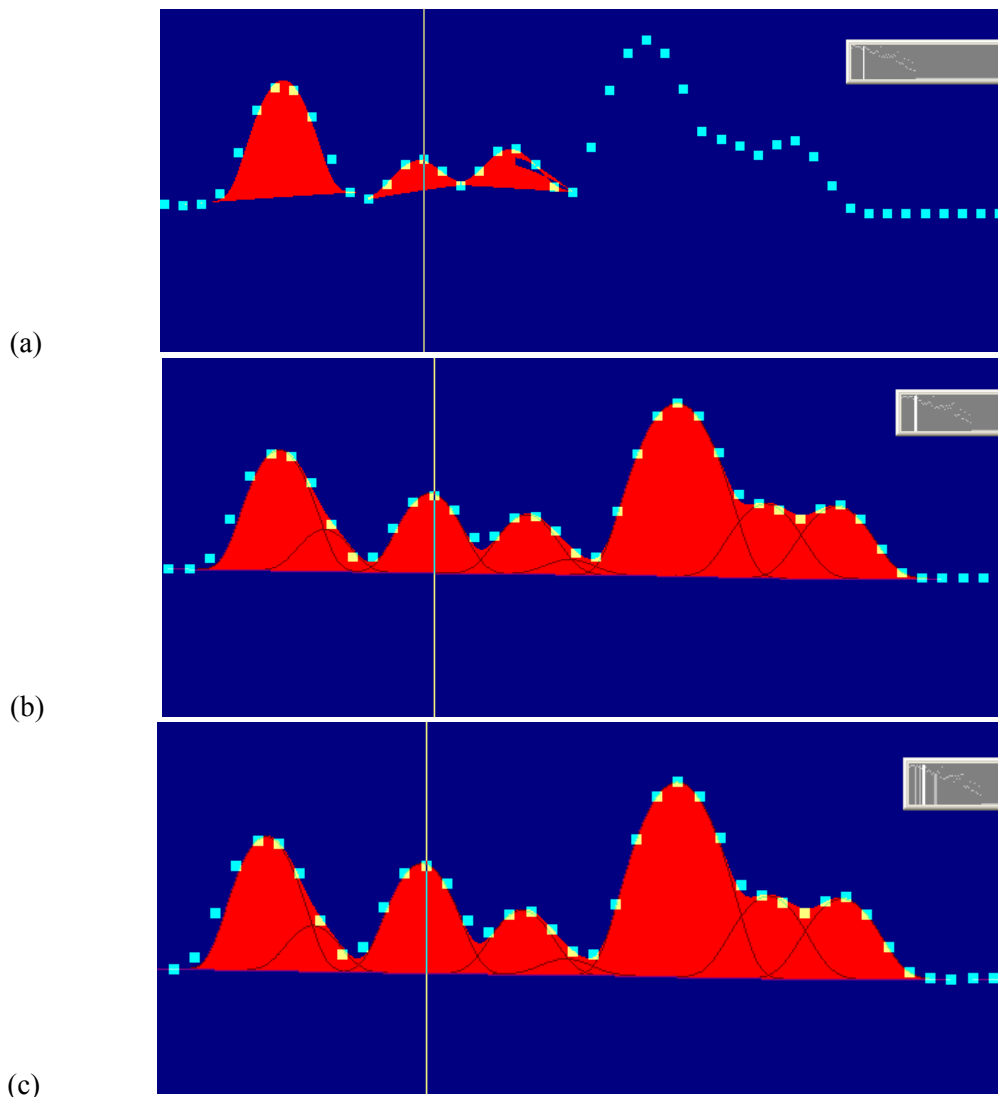


Figure 3.5 Cs-137 661.7 keV peak interference at (a) 20,000 MWD/MTU, (b) 50,000MWD/MTU, and (c) 80,000 MWD/MTU. (peak with marker is 661.7 keV)

To quantify this uncertainty introduced by interference from neighboring gamma peaks for counting of the Cs-137 peak, other MCNP calculations were performed with these interference gamma peaks removed artificially from the neighboring region. Computer program was written to estimate the net peak areas of Cs-

137 661.7 keV without interference. Comparing the net peak areas of Cs-137 peak with and without interference can quantitatively define the uncertainty in Cs-137 peak counting caused by gamma spectral-interference. The results are given in Table 3.5, which shows that due to the interference from other radionuclides, measuring the full energy peak of Cs-137 661.7 keV line will introduce large error at the beginning of fuel cycle. Although the effect of interference alleviates with burnup, it still causes about 9% uncertainty in measurement at the discharge burnup (80,000 MWD/MTU). For comparison, the statistical uncertainties for the net peak area listed in Table 3.5 are all less than 0.01%.

Table 3.4 Cs-137 Gamma Peak Interference

Radio-nuclide	Energy (keV)	Half-life
Ag-110m	657.57	249.8d
Nb-97	657.92	1.23h (Zr97, 16.8h)
I-132	659	2.28h (Te132, 3.2d)
Cs-137	661.62	30.07y
Ce-143	664	1.377d
Te-131m	665.05	1.35d
I-132	667.69	2.28h (Te132, 3.2d)

Table 3.5 Cs-137 661.7 keV Net Peak Area Interference Bias

Burnup	Net Peak Area (Counts)		Interference Bias
	No interference	With Interference	
20,000 MWD/MTU	$1.07 \times 10^8$	$0.67 \times 10^8$	37%
50,000 MWD/MTU	$2.31 \times 10^8$	$1.71 \times 10^8$	27%
80,000 MWD/MTU	$3.22 \times 10^8$	$2.95 \times 10^8$	9%

### 3.3.4.3 Error Analysis for Using Cs-137 Full Energy Peak as a Burnup Indicator

Once the full energy peak area of a characteristic gamma peak is determined from the measured spectrum, the activity of its emitter is calculated by:

$$A = \frac{C}{\Gamma \varepsilon T} \quad (3.6)$$

where A is the activity; C is the net peak area counts;  $\Gamma$  is the branching ratio for the gamma line; T is the counting time period; and  $\varepsilon$  is the full peak energy efficiency.

To use Cs-137 as a burnup indicator, one needs to determine the net peak area counts for the 661.7 keV line, then calculate the activity of Cs-137 by Equation 3.6. As the activity is derived, the burnup can be determined from the relationship presented in Figure 3.4. During this process, several components will introduce error to the final prediction of fuel burnup.

The first component of uncertainty is coming from the net peak area counts. This component is attributed by the error caused by interference and the statistical error for the peak area. As just discussed, generally, statistical error is negligible. The second component of uncertainty is contributed by  $\varepsilon$ , the absolute efficiency obtained from absolute efficiency calibration. In practice, obtaining an absolutely calibrated efficiency curve with high accuracy for the prototype detection system is not easy. The monoenergetic standard used to

calibrate the system has to be prepared as a uniformly distributed Cs-137 source mixed in UO<sub>2</sub> matrix with similar construction to a typical fuel pebble. The third component of uncertainty is the branching ratio. The relative error of this term is estimated to be 0.2% (based on ENSDF data). In addition to all the above, the last uncertainty component is introduced by power history variation of fuel pebble in the core. All of these components are listed in Table 3.6.

Table 3.6 Error Components for Cs-137 Full Energy Peak

Uncertainty Components	20,000 MWD/MTU	50,000 MWD/MTU	80,000 MWD/MTU
Peak Area Interference	± 37%	± 27%	± 9%
Peak Area Statistic	±0.1%	± 0.1%	± 0.1%
Absolute Efficiency Calibration	± 5%	± 5%	± 5%
Branching Ratio	± 0.2%	± 0.2%	± 0.2%
Power History	± 1.46%	± 1.02%	± 0.86%
Total	± 37.76%	± 26.50%	± 9.94%

### 3.4 Evaluation of Relative Activity Burnup Indicators

#### 3.4.1 On-line Self-calibration of Relative Efficiency

The burnup of irradiated fuel can also be determined from the activity ratios of two radionuclides. The activity ratio is derived from the net peak areas, branching ratios, and the relative efficiency of two gamma lines by

$$R = \frac{A_i}{A_j} = \frac{C_i \varepsilon_j \Gamma_j}{C_j \varepsilon_i \Gamma_i} \quad (3.7)$$

The advantage of using the activity ratio is that there is no need to know the absolute detection efficiency for each gamma line, because only the relative efficiency ratio  $\varepsilon_j/\varepsilon_i$  is required. This allows for the consideration of an efficiency self-calibration scheme for the burnup detector, which greatly simplifies the operational requirements of the monitor. To achieve that, we searched for potential radionuclides, which would exist in each irradiated pebble and could serve as built-in relative calibration standards. Clearly, such a standard should emit a series of gamma-rays over a wide energy range, its gamma energy peaks should be easily identified from the spectrum (strong activity, strong gamma intensity, no interference, etc.), the gamma intensities of its energy peaks are accurately known (to less than 1% error if possible), and have a long half-life compared to the measurement time period. Using these criteria, we identified I-132, Cs-134, and La-140 as candidates for the self-calibration operation. For the relative efficiency self-calibration, the activity ratio of two gamma lines is unity since both gamma lines are emitted from the same radionuclide, therefore, the relative efficiency can be determined as:

$$\frac{\varepsilon_i}{\varepsilon_j} = \frac{C_i \Gamma_j}{C_j \Gamma_i} \quad (3.8)$$

To examine the suitability of these radionuclides for efficiency calibration, a computer experiment was performed using the pebble/spectrometer MCNP model that was described earlier. Initially, an absolute efficiency curve was constructed using monoenergetic source simulations in the energy range 300 – 3000 keV. Subsequently, the pebble's spectrum (e.g., at 20,000 MWD/MTU) was used to construct the absolute

efficiency curve using the gamma lines of I-132, Cs-134, and La-140. Figure 3.6 shows a comparison of the results obtained in both cases. In general, good agreement is observed between the efficiency values obtained using the two different methods. This confirms that these radionuclides can be used in the relative calibration task. Nevertheless, La-140 presents the best coverage of the energy range. Therefore, it was selected as the radionuclide to be used in the relative calibration operation.

Next, the method developed by Hawari et al. [4] was implemented to construct the relative efficiency curve using a radionuclide that emits a series of gamma rays (e.g., La-140). In this case the relative efficiency curve of an HPGe is assumed to vary as

$$\ln\left(\frac{\varepsilon_i}{\varepsilon_0}\right) = f\left(\ln\left(\frac{E_i}{E_0}\right)\right) \quad (3.9)$$

Therefore, for any two gamma lines designated  $i$  and  $j$ , and upon expansion the above equation can be written as

$$\ln\left(\frac{\varepsilon_i}{\varepsilon_j}\right) = \sum_{k=0}^N a_k \left( \ln^k\left(\frac{E_i}{E_0}\right) - \ln^k\left(\frac{E_j}{E_0}\right) \right). \quad (3.10)$$

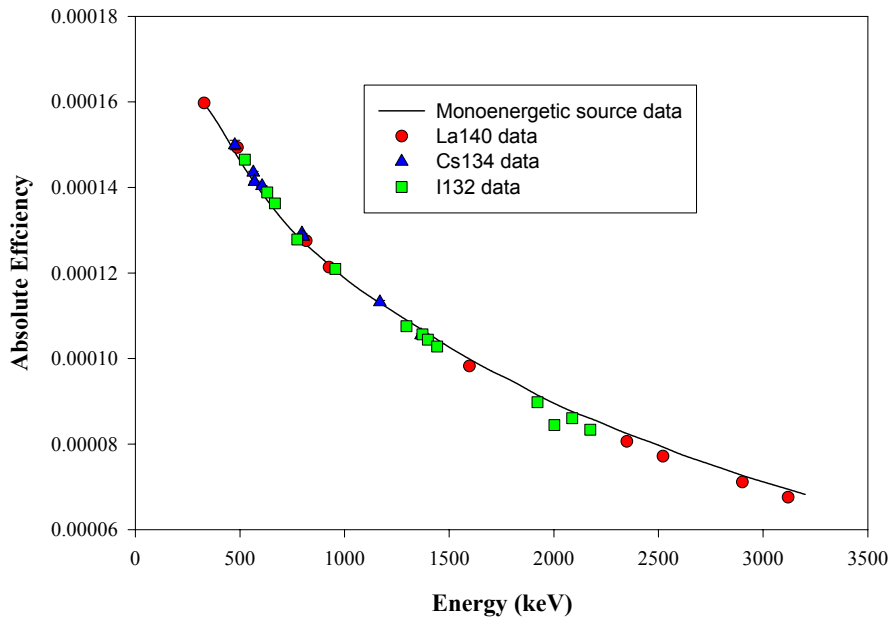


Fig 3.6. The absolute efficiency curve of the gamma-ray spectrometer.

Further analysis results in establishing that the relative efficiency curve actually varies as a power of the relative energy, where the power is actually a function of energy. Figure 3.7 shows the efficiency data points relative to the 3119 keV gamma line of La-140 obtained from the calculated absolute efficiency values as compared to the curve obtained using the fitting approach. Notice that in a physical measurement situation no absolute efficiency values would be available. Therefore, the only approach to construct the relative curve would be to extract relative efficiency data from the measured gamma spectrum of a fuel pebble and then apply the method described above.

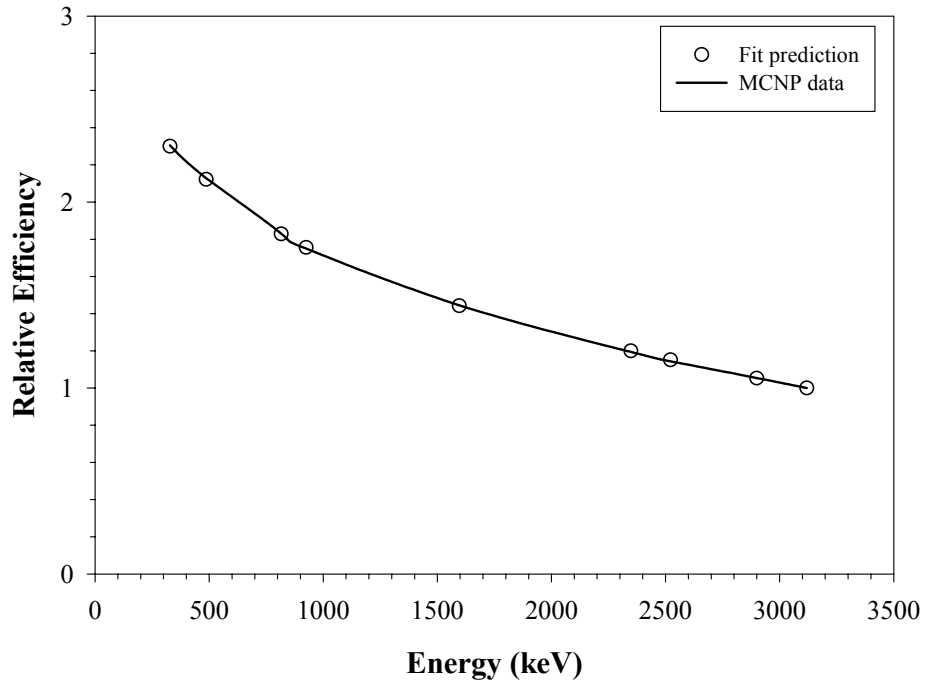


Fig 3.7. The relative efficiency curve of the gamma-ray spectrometer.

### 3.4.2 Evaluation of Using $^{134}\text{Cs}/^{60}\text{Co}$ as Burnup Indicator

Co-60 has two well known gamma peaks with strong intensities (1173.2 keV with 99.97% and 1332.5 keV with 99.98% intensities), these two peaks can be used in the fuel burnup measurement by doping the fuel pebble with small amount of Co-59 to utilize the Co-59 ( $n, \gamma$ ) Co-60 reaction. The ratio of  $^{134}\text{Cs}/^{60}\text{Co}$  is discovered to have a good correlation with fuel burnup.

Cesium-134 is produced by neutron capture on the fission product Cs133; therefore, its production requires two neutron interactions. The first is the neutron that causes fission of the uranium or plutonium, and the second is the Cs-133 ( $n, \gamma$ ) Cs-134 reaction. Because these interactions are the primary source of Cs-134, the concentration of Cs-134 within the fuel is approximately proportional to the square of the integrated flux. While Co-60 produced from fission is negligible, therefore, the Co-60 produced within the fuel is primarily from Co59 ( $n, \gamma$ ) Co-60 reaction, which is proportional to the integrated flux. Hence, by dividing the concentration of Cs-134 by the concentration of Co-60, the ratio becomes approximately proportional to the burnup. The correlation of burnup with  $^{134}\text{Cs}/^{60}\text{Co}$  is plotted in Figure 3.8. The interference check was performed for both Cs-134 and Co-60. It found that the Co-60 1173.2 keV peak is contaminated by I-132, which also emits 1173.2 keV gammas. However, the Co-60 1332.5 keV peak and Cs-134 604.7 keV peak remain free of interference. These two peaks can be identified clearly from the fuel pebble spectrum. Therefore, the  $^{134}\text{Cs}/^{60}\text{Co}$  ratio can be used as a burnup indicator. The peak regions of Cs-134 and Co-60 in the fuel pebble spectrum are shown in Figure 3.9. The error analysis for using  $^{134}\text{Cs}/^{60}\text{Co}$  to predict fuel burnup was performed too and the results are listed in Table 3.7.

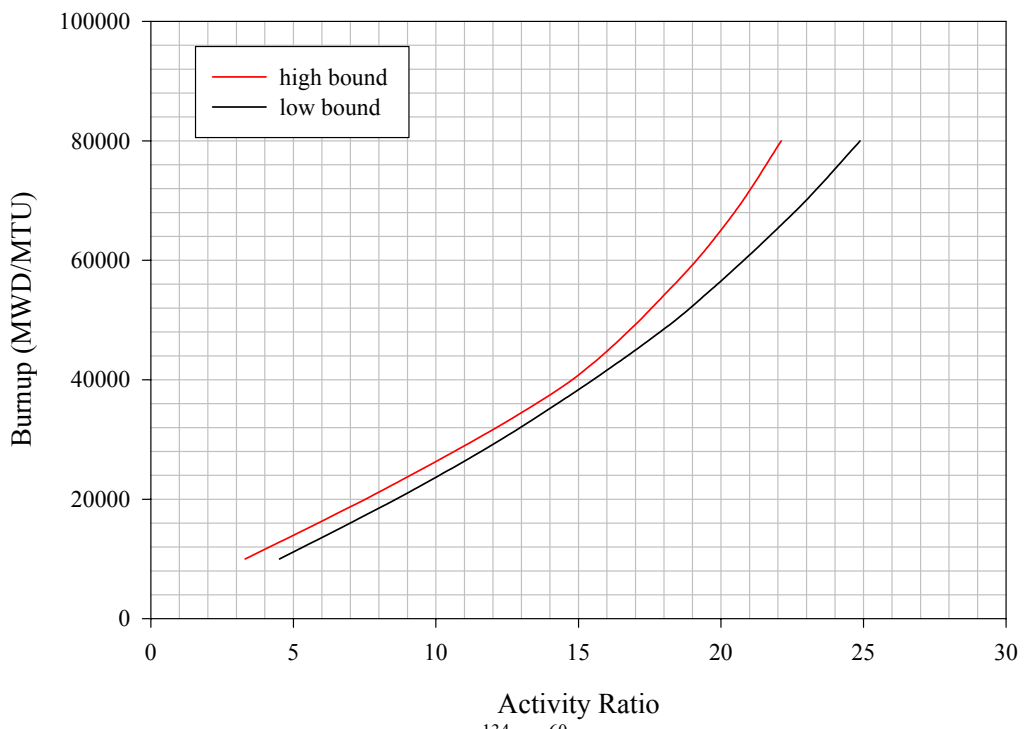


Figure 3.8 Burnup vs.  $^{134}\text{Cs}/^{60}\text{Co}$  Activity Ratio Correlation

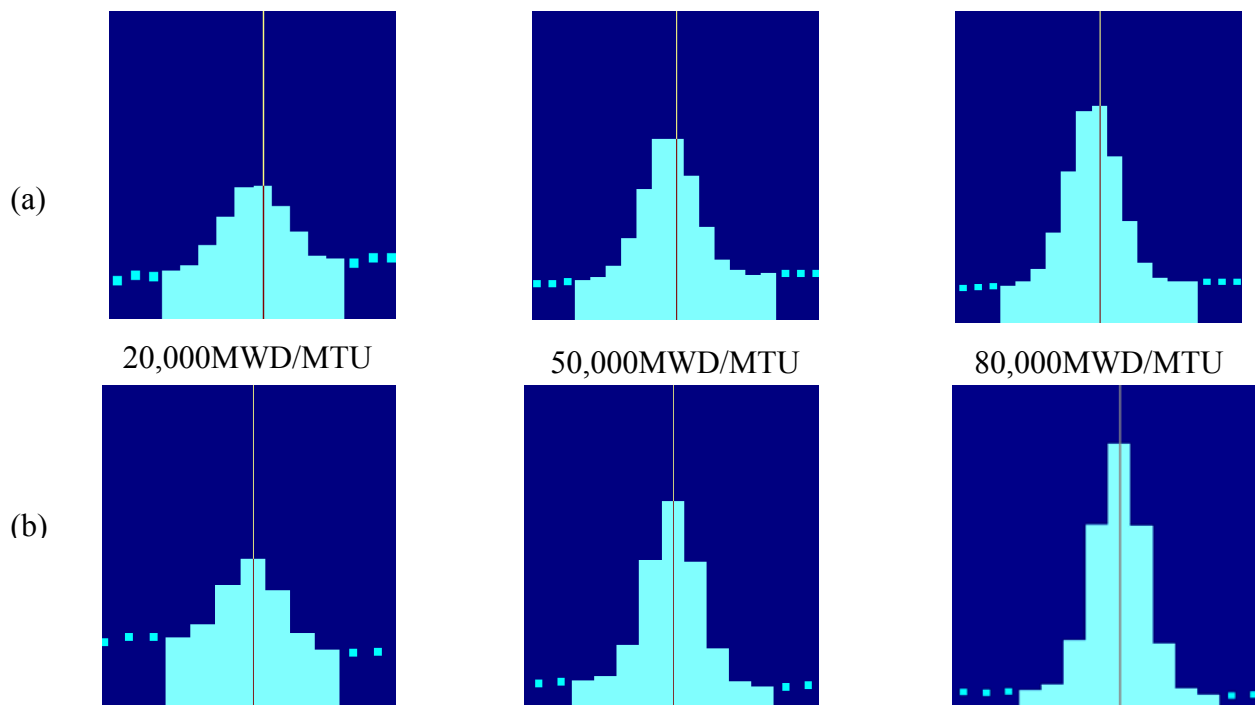


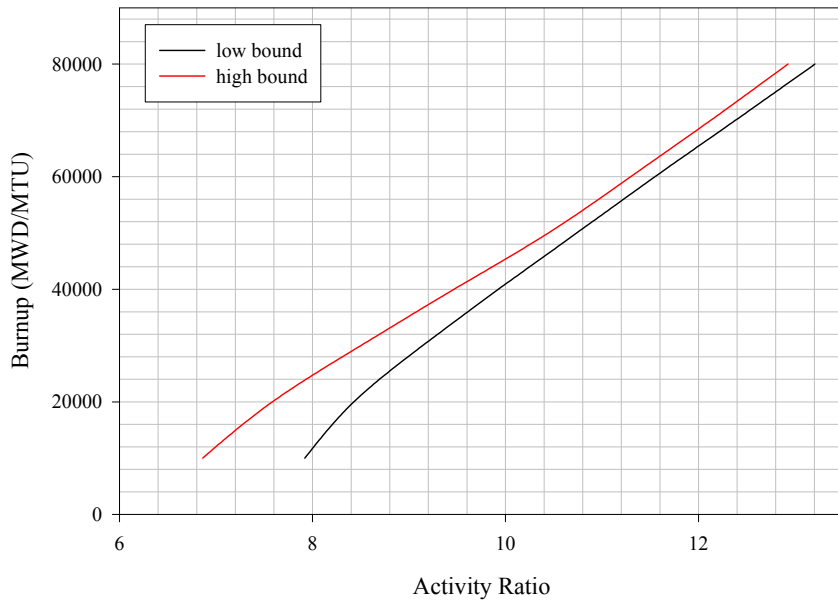
Figure 3.9 Co-60 1332.5 keV peak (a) and Cs-134 604.7 keV peak (b) in fuel pebble spectra at different burnup steps

Table 3.7 Error Components for  $^{134}\text{Cs}/^{60}\text{Co}$  Ratio

Uncertainty Components	20,000 MWD/MTU	50,000 MWD/MTU	80,000 MWD/MTU
Peak Area Interference	$\pm 0\%$	$\pm 0\%$	$\pm 0\%$
Peak Area Statistic	$\pm 0.1\%$	$\pm 0.1\%$	$\pm 0.1\%$
Relative Efficiency Calibration	$\pm 1.6\%$	$\pm 1.6\%$	$\pm 1.6\%$
Branching Ratio	$\pm 0.047\%$	$\pm 0.047\%$	$\pm 0.047\%$
Power History	$\pm 2.22\%$	$\pm 1.18\%$	$\pm 1.96\%$
Total	$\pm 2.74\%$	$\pm 1.99\%$	$\pm 2.53\%$

### 3.4.3 Evaluation of Using a Built-in Relative Burnup Indicator

It is possible to find radionuclide pairs produced within the fuel during irradiation that could give a good correlation with burnup independent of power history. These radionuclide pairs must also have strong, clear gamma lines to be used in gamma-ray spectroscopy analysis. There are a total of 58,996 radionuclide pairs that can be constructed out of the 344 non-zero activity radionuclides generated by the ORIGEN2 depletion calculation. To investigate the feasibility of using built-in relative burnup indicators, a program was written in C++ to perform the search on the ORIGEN2 output. The criteria used to perform the absolute activity burnup indicator search can also be applied here. For each ratio pair, it should have a monotonous increase or decrease relationship with burnup; it should have a difference greater than 5% between each burnup step, and the error introduced by power history variation should be less than 15%. There are a total of 4,570 ratio pairs constructed by 267 radionuclides that passed this search. After performing interference and MDA checks on these radionuclides, 24 ratio pairs were identified. Among these ratio pairs,  $^{239}\text{Np}/^{132}\text{I}$  was selected to be the best since both of them have very strong and clean gamma peaks.

Figure 3.10 Burnup vs.  $^{239}\text{Np}/^{132}\text{I}$  Activity Ratio Correlation

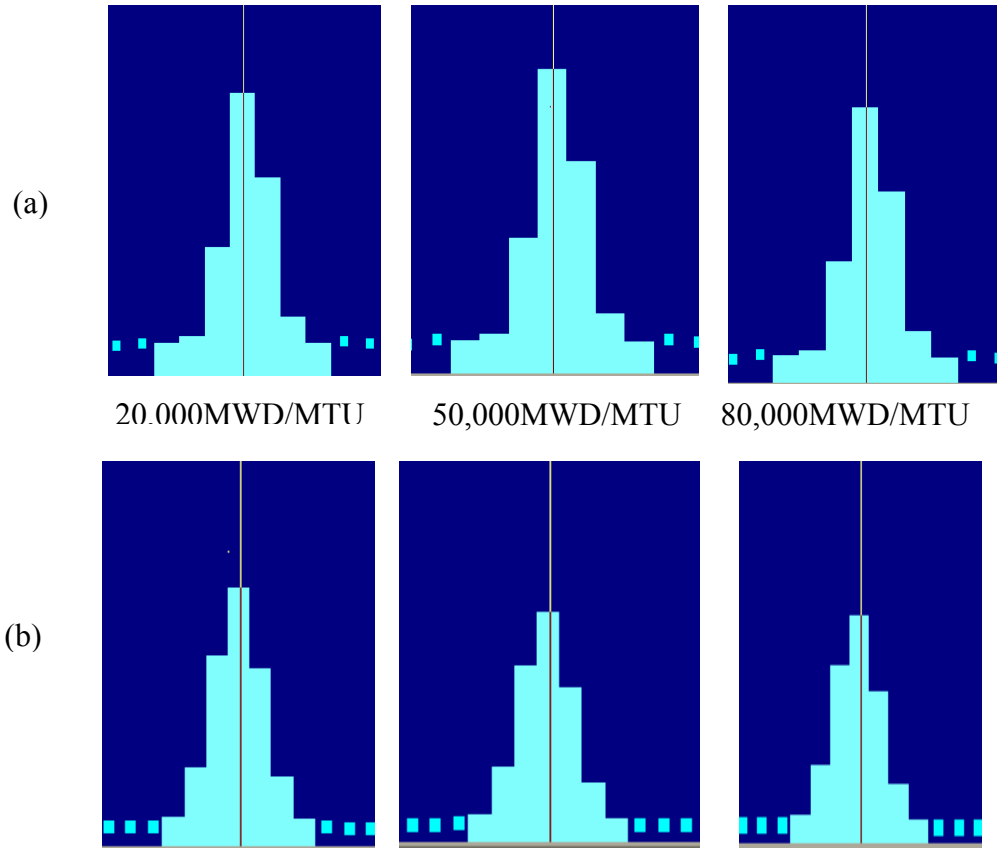


Figure 3.11 Np-239 334 keV peak (a) and I-132 630 keV peak (b) in fuel pebble spectra at different burnup steps

The correlation of  $^{239}\text{Np}/^{132}\text{I}$  with burnup is shown in Figure 3.10 and their gamma peaks are shown in Figure 3.11. The error analysis was derived for  $^{239}\text{Np}/^{132}\text{I}$  using similar approach as for the Cs-137 and  $^{134}\text{Cs}/^{60}\text{Co}$  ratio method and the results are listed in Table 3.8.

Table 3.8 Error Components for  $^{239}\text{Np}/^{132}\text{I}$  Ratio

Uncertainty Components	20,000 MWD/MTU	50,000 MWD/MTU	80,000 MWD/MTU
Peak Area Interference	$\pm 0\%$	$\pm 0\%$	$\pm 0\%$
Peak Area Statistic	$\pm 0.1\%$	$\pm 0.1\%$	$\pm 0.1\%$
Relative Efficiency Calibration	$\pm 1.5\%$	$\pm 1.5\%$	$\pm 1.5\%$
Branching Ratio	$\pm 2.27\%$	$\pm 2.27\%$	$\pm 2.27\%$
Power History	$\pm 1.76\%$	$\pm 0.46\%$	$\pm 0.36\%$
Total	$\pm 3.24\%$	$\pm 2.76\%$	$\pm 2.75\%$

### 3.5 Random Summing Simulation

Pulse pileup effect was also investigated. Since fuel pebbles are expected to have activities on the order of

thousands of Ci, the proper design of the measurement system requires an assessment of its performance under high count rate conditions. Under such conditions, pulse pileup (i.e., random summing), if not accounted for, may result in distorting any collected gamma spectrum. Consequently, we developed a Monte Carlo computer routine that utilizes the random interval distribution function (based on Poisson statistics) to predict the effect of pileup. Combining with the pile-up logic, a recursive digital convolution algorithm was implemented to simulate the pile-up behavior of a digital gamma-ray assay system. Since digital systems can have throughputs greater than  $10^5$  cps, such a system is expected to be the one used in an on-line burnup measurement device. In this simulation, opposed to traditional analog systems, where the output of an amplifier is digitized to produce the counting signal, digital pulse shaping is based on digitizing the pre-amplifier pulse and using mathematical algorithms (filters) to produce pulse shapes that are difficult to obtain with analog systems. In our particular case, we passed the digitized preamplifier pulses through filters that produce trapezoidal pulses. Figure 3.12 shows a typical result on the effect of pulse pileup for the equivalent of a  $2\ \mu\text{s}$  shaping time. Using this code, we are able to optimize the counting setup for a proposed assay device by including, in addition to other aspects, the count rate dependent response of the system

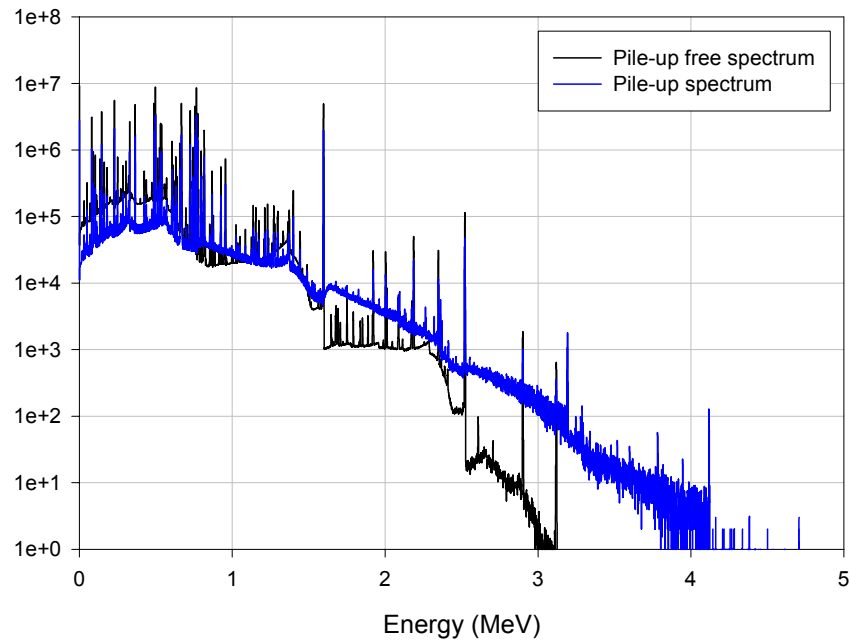


Fig. 3.12. The effect of random summing (pile-up) on the gamma-ray spectrum

### 3.6 Construction of a Gamma-Spectrometry Detection System and Demonstration

A Gamma spectrometry measurement system was constructed. The main components of the system are: a 40% n-type coaxial HPGe (resistant to neutron damage), a digital gamma-ray spectrometer, and a data acquisition computer. The experimental verification for the gamma spectrometry measurement was performed on the spent fuel at the NC State PULSTAR reactor. To make the measurement system be able to scan the irradiated fuel assembly that is underneath water, a railway was built spanning the PULSTAR reactor pool, with the detector being put up facing down on a cart which can roll over the railway. The detector is surrounded by a lead shielding, and a collimator is extended from the detector to the fuel assembly 12 feet underneath the water to reduce background. This experimental setup is shown in Fig. 3.13.

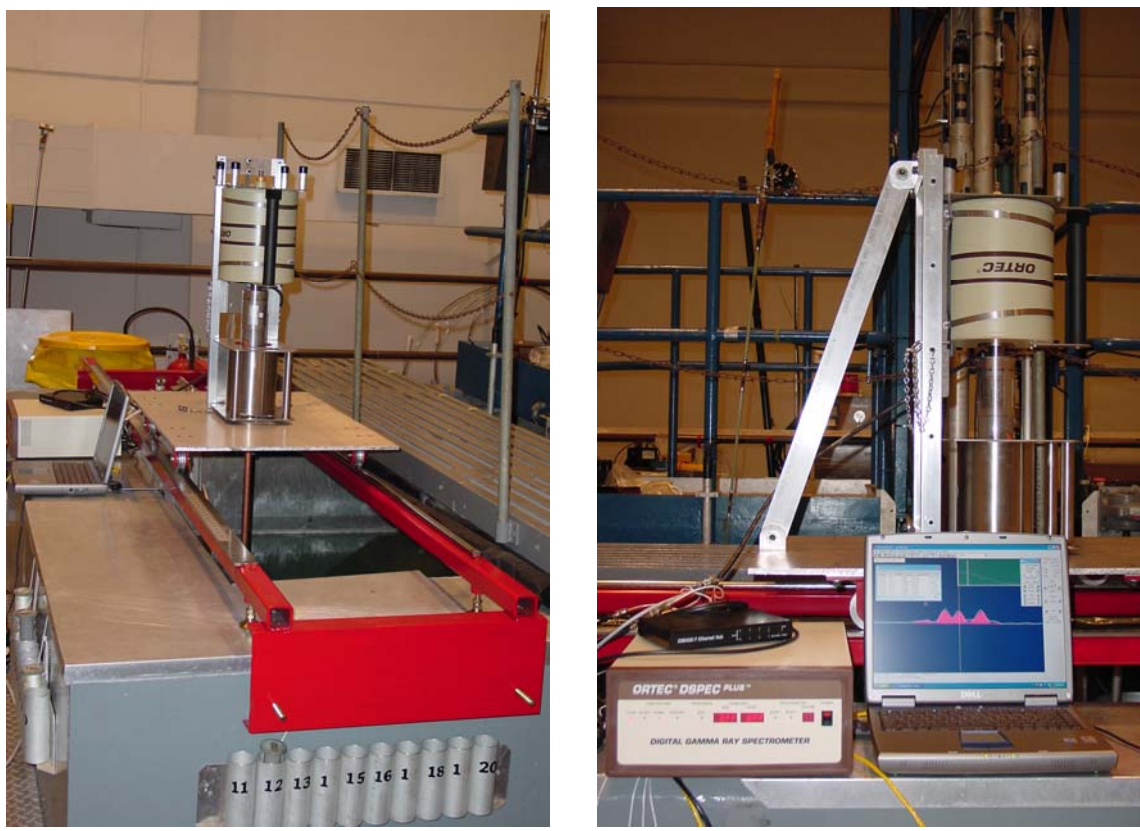


Figure 3.13 Experimental Setup

Two major measurements were performed: one was measuring the irradiated spent fuel to simulate the high burnup fuel pebble; and the other was measuring the irradiated fresh fuel to simulate the low burnup fuel pebble. For the irradiated spent fuel measurement, the fuel assembly was irradiated in the PULSTAR core for 3 hours at the 500 kW power level. Then the fuel assembly was measured after about 21 hours of cooling time. For the irradiated fresh fuel assembly measurement, the fresh fuel assembly was irradiated at 250 kW for one hour and then was measured after 2 hours of cooling time.

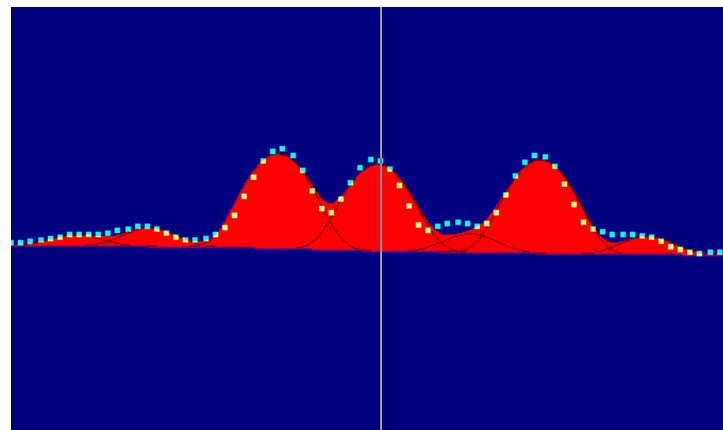


Figure 3.14 Cs-137 peak interfered by Nb-97, I-132, and Ce-143 observed from the experiment spectrum (marker points Cs-137 peak)

Figure 3.14 – 3.16 shows the gamma peaks of Cs-137, La-140, Np-239, I-132, and Cs-134 in the measured spectrum from irradiated spent fuel spectrum. For the irradiated fresh fuel, since the irradiation time is short, little Cs-137 and La-140 are produced. However, for the short lived ones, like Np-239, I-132, their peaks can be seen from the irradiated fresh fuel spectrum. These observations are consistent with the simulation predictions described earlier.

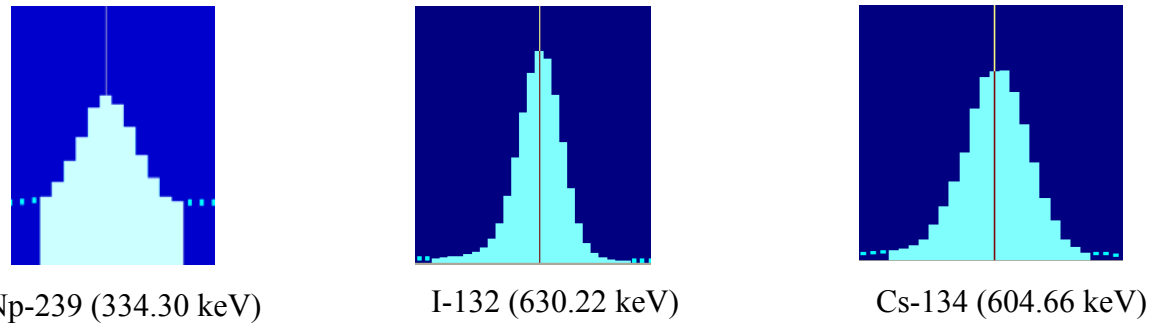


Figure 3.15 Np-239, I-132, Cs-134 peaks observed from the experiment spectrum

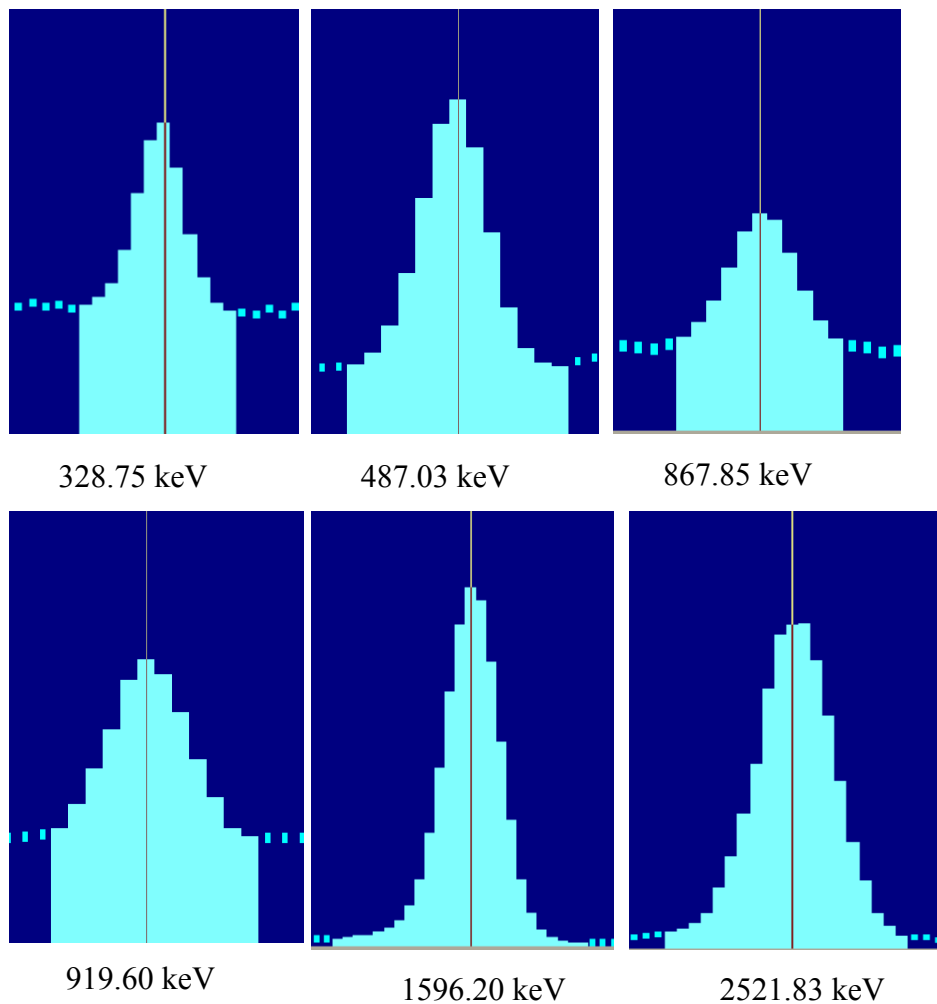


Figure 3.16 La-140 peaks observed from the experiment spectrum

## 4. BURNUP MEASUREMENT BY NEUTRON COUNTING

Although this project primarily focused on design a gamma spectrometry based burnup monitor system for MPBR, the feasibility of using passive neutron counting method for the on-line burnup measurement was also investigated. The difficulties with the neutron counting approach include low neutron emission rate, short measurement time (30 seconds), and extremely high gamma noise. Three questions on passive neutron counting were addressed in this project: (1) Is neutron emission a burnup indicator? (2) Can neutron emission be measured accurately within 30 seconds? and (3) Is neutron signal distinguishable from gamma noises? The results are summarized in the following sections.

### 4.1 Correlation between neutron emission and Burn up

Pebbles having been exposed to neutron flux in reactor core become neutron sources through decay of actinides and  $(\alpha, n)$  reactions. The first question for neutron counting approach is whether there is an acceptable correlation between neutron emission rate and fuel burn up. Neutron emission rate can be computed as a function of a depletion process by ORIGEN2. ORIGEN2 calculations show that for a typical PBR fuel burnup process:

- There are two major neutron sources within an irradiated pebble:  $(\alpha, n)$  neutrons and spontaneous fission neutrons;
- Both  $(\alpha, n)$  and spontaneous neutron emission rates increase with the burnup;
- The total neutron emission rate is in the order of  $10^4$  n/s at the discharge burnup (80,000MWD/MTU);
- Spontaneous neutron source is dominant. It contributes to 90% of total neutron emission at the discharge burnup;
- Major  $(\alpha, n)$  neutron emitters are Cm-242, Cm-244, and Pu-238;
- Major spontaneous neutron sources are Cm-242, Cm-244, and Cm-246;
- At the discharge burnup, Cm-242 and Cm-244 contribute 99% of total spontaneous neutrons or 89% of total neutrons.

Because Cm-244 is a major neutron source (contributing 75% of total neutron emission) and has a long half-life of 18.1 years, it is possible that the total neutron emission rate can be used as a burnup indicator (of course spontaneous fission neutron emission rate is a better burnup indicator; but distinguishing spontaneous fission neutrons from  $(\alpha, n)$  neutrons would cause additional difficulty in measurement so that approach was not pursued). Various analyses were done to establish the correlation between neutron emission and burnup and estimate its uncertainty.

#### (1). Library update

ORIGEN2 does not have cross section libraries for Pebble Bed Reactor (PBR). Analysis shows that for the same depletion process, neutron emission rate exhibits a large discrepancy for different reactor types (such as LWR and CANDU) at high burnups. To minimize the uncertainty in the depletion correlations for PBR, we updated ORIGEN2 cross section libraries using the same energy spectrum as discussed in Section 3. Ideally, one should use that energy spectrum to produce a complete set of one-group cross sections for PBR. However, ORIGEN2 cross section libraries contain more than one thousand nuclides; producing new cross sections for all the nuclides seems impractical and too time-consuming. Since we are only interested in

neutron emission, we chose to identify the nuclides that are important to neutron emission and only update the cross sections of these selected nuclides in a built-in library (such as that of PWR) and then use it as an approximate PBR library.

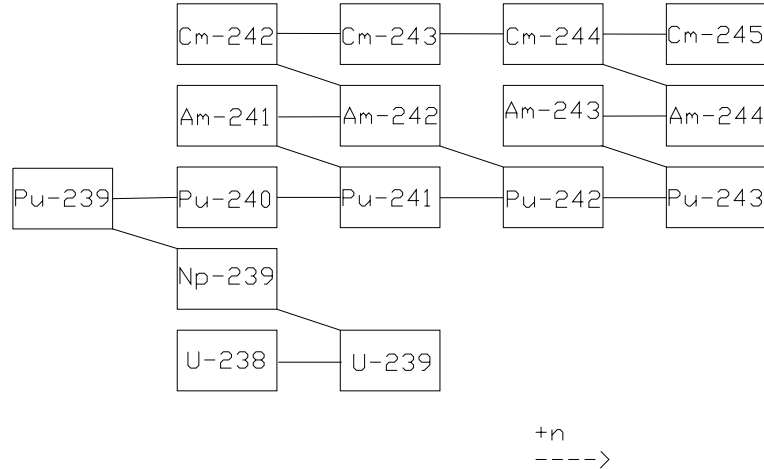


Figure 4.1. Cm-242 and Cm-244 formation chain

Specifically, analysis shows that Cm-242 and Cm-244 are the dominant neutron sources and they are produced through a series of neutron captures and beta decays. Figure 4.1 illustrates the formation chain of all the major actinides that are important to neutron emission. We decided to update the cross sections only for those nuclides. Unfortunately, four of them are not available in the ENDF databases so we could not generate one-group cross sections using the PBR energy spectrum. Cross sections of all of the other nuclides in the chain were replaced in the ORIGEN2 libraries by those computed by the PBR energy spectrum at the medium burned (50,000MWD/MTU) condition.

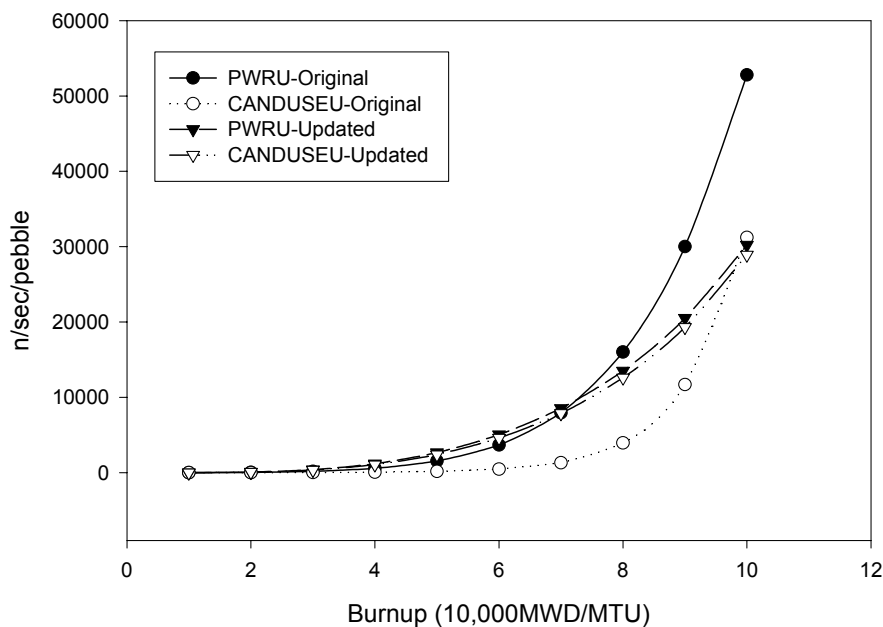


Figure 4.2 Burnup vs. total neutron emission for different libraries

To verify such modification is sufficient for the neutron emission consideration, we updated the  $(n, \gamma)$  and  $(n, \text{fission})$  cross sections of these nuclides in a PWR library PWRU and a CANDU library CANDUSEU as well as in the ORIGEN main program. Both the updated and original libraries were used in ORIGEN 2 calculations for a typical depletion process:  $\text{UO}_2$  fuel, 8% U-235, 100MW/MTU burnup rate, 1 day of cooling time after each 100 day (100,000MWD/MTU) with total 10 cycles. The results are plotted in Fig. 4.2, which shows that the original PWRU and CANDUSEU libraries yield significantly different neutron emission rates, with relative difference as high as 90%; while the two updated libraries produce very close results for neutron emission rate with the maximum relative difference less than 10%. This comparison proves that the update is sufficient and either of the updated libraries can be treated as an approximate PBR library in terms of the calculation of neutron emission. Such treatment may produce up to 10% uncertainty in neutron emission.

Table 4.1. Cross sections for PBR core loaded with fresh, medium and high burnt pebbles

Radionuclides	Fresh Core		Medium Burnup		High Burnup	
	n-r	n-f	n-r	n-f	n-r	n-f
92-U-235	20.7	99.3	20.2	96.4	22.7	111
92-U-238	3.46	0.0282	3.57	0.0296	3.40	0.0265
93-Np-239	26.3	0.21	26.3	0.218	27.2	0.195
94-Pu-239	249	406	235	385	271	444
94-Pu-240	336	0.277	292	0.276	274	0.250
94-Pu-241	123	330	118	316	136	366
94-Pu-242	36.4	0.149	36.6	0.155	33.5	0.139
95-Am-241	380	2.42	360	2.31	405	2.56
95-Am-243	67.4	0.201	68	0.207	64.6	0.190
96-Cm-242	6.04	0.599	6.06	0.588	6.17	0.657
96-Cm-244	18.2	0.604	18.9	0.624	17.5	0.586

## (2). Variation of cross sections

The update of cross sections for PBR was based upon the energy spectrum obtained at the medium burnup condition. The rationale for that is that due to the feature of random, continuous, multi-pass fuel circulation of fuel pebbles through the core, it is more likely to have an equilibrium core that contains pebbles of all burnup levels; but the average burnup of all fuel pebbles remains almost a constant. In addition, it has been shown that the energy spectrum in a pebble is more dependent on the burnup levels of the surrounding pebbles rather than the burnup level of itself. Therefore, using the energy spectrum at the medium burnup to generate one-group cross sections seems to a good approximation. Of course, the neutron energy spectrum within a pebble definitely fluctuates as it travels in the core and its burnup level changes; that will in turn cause the fluctuation in the one-group cross sections. To evaluate the effect of such fluctuation on the neutron emission/burnup correlation, we also updated the PWRU library by PBR cross sections obtained for a fresh and high burnup core and then ran the same ORIGEN2 calculations. The one group cross sections at different burnup conditions are given in Table 4.1 and the ORIGEN2 results are plotted in Fig. 4.3. As shown, the spectrum-averaged cross sections can vary as much as 10% with different burnup conditions, which leads to about 18% change in neutron emission at 80,000MWD/MTU. Due to the complex nature of the problem involved, it is reasonable to assume that any computed spectrum-averaged cross sections for PBR fuel

pebbles may have few percent (such as 5-10%) of uncertainty. Therefore, it is concluded that such uncertainty in the determination of average cross sections may lead to up to 18% of uncertainty in the neutron emission rate at the high burnup levels.

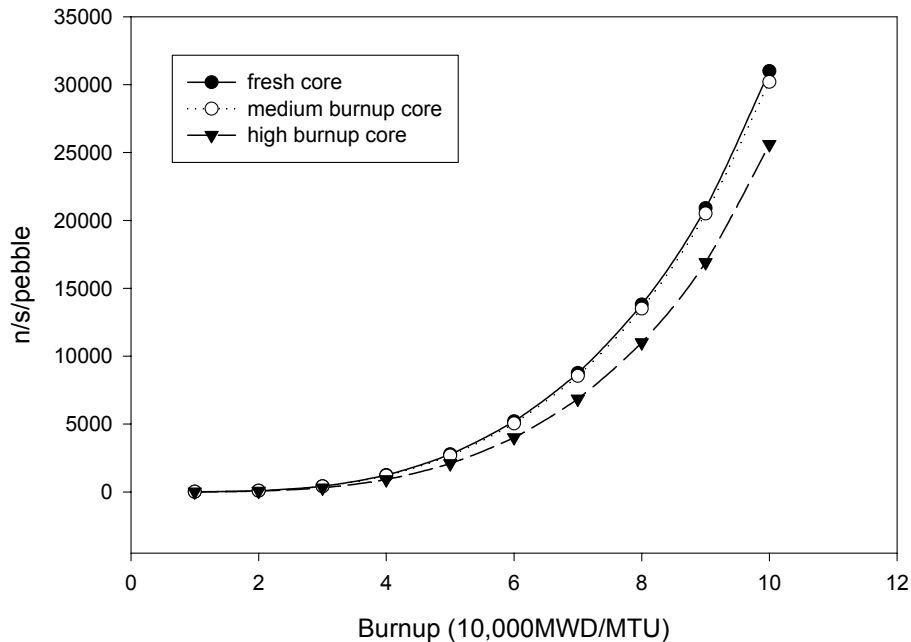


Fig. 4.3 Neutron emissions vs. variation of cross sections

### (3). Variation of burnup rate

In the above calculations, it was always assumed that a pebble is burnt with a constant and average burnup rate, 100 MW/MTU. Once again, due to the feature of random, continuous, multi-pass circulation of fuel pebbles through the core, even when the reactor is operated at a constant power, the neutron flux experienced by a pebble (i.e., its burnup rate) keeps changing as it moves through the core. There are infinite numbers of different burnup histories so it is impossible to simulate all of them. To estimate the effect of different burnup histories on the neutron emission, we selected an upper limit and a lower limit for the burnup rate to examine how the neutron emission rate changes with the burnup rate. Considering the core configuration and the fundamentals of reactor physics, we chose 50MW/MTU and 150MW/MTU as the two limits and run the ORIGEN2 calculations by assuming that pebbles are burnt constantly at a lower rate of 50MW/MTU (50% lower than the average rate) or at a higher rate of 150MW/MTU (50% higher than the average rate) during their lifetime.

Figure 4.4 compares the total neutron emission rates at given burnup levels for different burnup rates: 50, 100, and 150 MW/MTU. Results demonstrate that neutron emission rate also depends upon the burnup rate. At the discharge burnup 80,000MWD/MTU, the relative difference on neutron emission rate is about 15%. This value can be used to quantify the uncertainty in neutron emission rate caused by different burnup histories.

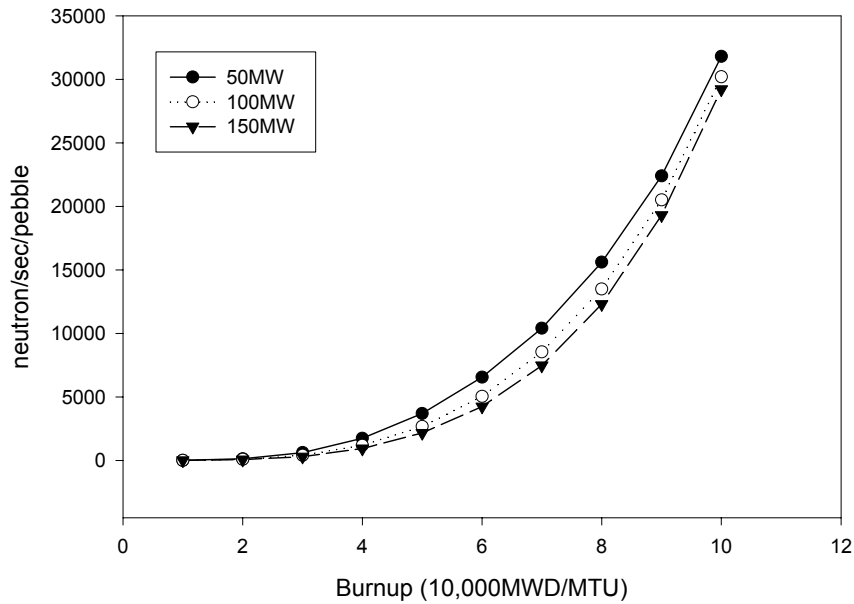


Figure 4.4 Variation of neutron emission rate with burnup rate

#### (4). Variation of cooling time

An irradiated fuel pebble that just comes out of the reactor barrel is highly radioactive and is also very hot in temperature. It is usually designed to let pebbles to decay and cool for a period of time before measurement, because reducing radioactivity and temperature is helpful for measurement. The period of time prior measurement is called decay waiting time or cooling time. The cooling time changes significantly with different designs; normally this parameter varies from minutes to days. To evaluate its effect on the neutron emission rate, we ran ORIGEN2 simulations for the average depletion history using the following cooling times: 0, 30 minutes, 1 day, 2 days, and 4 days. Results show that neutron emission is very insensitive to this parameter. The relative difference among the neutron emission rates at the same burnup level is within 1% for all the cooling times that we used. Therefore, the selection of cooling time does not affect the neutron emission/burnup correlation much. In fact, this conclusion is expectable because the major neutron emitters (Cm-242 and Cm-244) have long half-lives.

#### (5). Variation of irradiation time step

The last factor we considered that may cause uncertainty in the neutron emission is a computational parameter. In the input file of ORIGEN2, one needs to input an irradiation time step for the depletion calculations of fuel pebbles. Irradiation time step of 100 days was previously used in our calculations. It turns out that the neutron emission rate depends upon the time step used in the calculations. To quantify the effect of this parameter, various irradiation time steps (25, 50, and 100 days) were used to reach the same burnup level. Results show that this parameter may cause an uncertainty of 2.5% in the neutron emission rate at the same burnup level.

## (6). Conclusion

Using the average burnup scenario, a correlation was built between total neutron emission and burnup level, which is shown in Fig 4.5. This correlation is expected to be used later in the burnup measurement for MPBR. For convenience, the neutron emission rate  $y$  (n/s/pebble) and burnup level  $x$  (in 10,000MWD/MTU) can be represented by a simple mathematical expression obtained by curve-fitting:

$$y = 8.30 \cdot x^{3.56}. \quad (4.1)$$

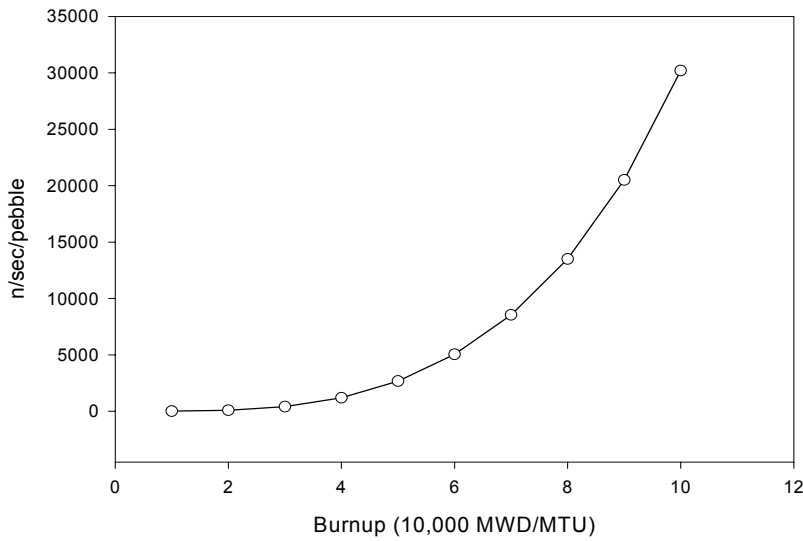


Fig. 4.5 Total neutron emission rate of a pebble at different burnup levels

Please note that this correlation was developed by using an incomplete PBR cross section library based upon a simplified model and by using an average irradiation history. For quantifying the uncertainty in this correlation, variation analyses were performed on using the incomplete library, cross section values, burnup rate, cooling time and irradiation time step. Around the discharge burnup level, the uncertainties in neutron emission rate caused by these variations were found to be 10%, 18%, 15%, 1.0% and 2.5%, respectively. Thus, the overall uncertainty in neutron emission rate can be estimated as

$$\sigma = \sqrt{0.1^2 + 0.18^2 + 0.15^2 + 0.01^2 + 0.025^2} \approx 26\%.$$

This large uncertainty is primarily attributed by assuming about 10% of changes in the spectrum-averaged cross sections and 50% of changes in burnup rate. In reality, such assumptions could be too conservative. If so, the uncertainty can be narrowed down. In addition, it should point out that this uncertainty (26%) was derived for high burnup region (around 80,000 MWD/MTU); at low burnup region (< 40,000 MWD/MTU), the uncertainty in the correlation is even larger.

In the burnup measurement, the correlation, Eq. (4.1), is used to determine pebble burnup level according to a

measured neutron emission rate. Due to the uncertainty in neutron emission, two pebbles that have exactly the same burnup level may exhibit different neutron emission rates and then subsequently are determined by the correlation as having two different burnup levels. The uncertainty in the burnup determination at the discharge burnup due to the uncertainty in neutron emission can be estimated accordingly.

The uncertainties in neutron emission and in burnup are expressed by  $\Delta y / y$  and  $\Delta x / x$ , respectively.

Because of

$$y' \approx \frac{\Delta y}{\Delta x},$$

we have

$$\Delta x = \frac{\Delta y}{y'}; \quad \text{and} \quad \frac{\Delta x}{x} = \frac{\Delta y}{xy'} = \frac{\Delta y}{y} \cdot \frac{y}{xy'}.$$

At the discharge burnup,

$$\begin{aligned} \frac{\Delta y}{y} &= 26\%; \\ y' &= 8.30 \cdot 3.56 \cdot x^{2.56} \\ \frac{y}{xy'} &= \frac{8.30 \cdot x^{3.56}}{8.30 \cdot 3.56 \cdot x^{3.56}} = \frac{1}{3.56} \end{aligned}$$

so the uncertainty in burnup determination caused by the uncertainty in neutron emission at 80,000MWD/MTU is given by:

$$\frac{\Delta x}{x} = \frac{26\%}{3.56} = 7.3\%.$$

That is, due to the super-linear nature of the correlation (see Fig. 4.5), the uncertainty in burnup determination is reduced. By this result, a pebble that has a real burnup of 80,000MWD/MTU can be determined within the range from 74,160 to 85,840 MWD/MTU, because of the uncertainty in neutron emission. Although not very satisfactory, such uncertainty is acceptable in a practical point of view. To narrow down the uncertainty, better modeling tools (such as using space-dependent and two-group depletion code) must be used to derive the correlation.

## 4.2 Detectability of neutron emission and detector system design

After the neutron emission/burnup relation is established, the next issue is to investigate the detectability of neutron emission for the on-line burnup measurement and design a detector system that meets the requirements.

### (1). Requirement on the detection efficiency

Based upon the MPBR design, one pebble comes out of the reactor barrel about every 30 seconds. Assuming there is only one burnup monitor built in the fuel handling loop (see Fig 1.1), the measurement must be done within 30 seconds in order to maintain the balance of the number of fuel pebbles in the reactor core. Because the neutron emission rate of a pebble is low and measurement time is short, detection efficiency of the neutron detector system must be high to perform the measurement in time. As shown in Fig. 4.5, the neutron emission rate is too low for accurate measurement within 30 seconds at low burnup levels. In addition,

uncertainty in neutron emission/burnup correlation at low burnup is much larger than that at high burnup. So it is impossible to achieve accurate burnup measurement by neutron counting at low burnup. For neutron detector system design, we require that the minimal detection efficiency should be such that it can limit the statistical uncertainty in neutron counts within 30 seconds to 5% at the discharge burnup. If possible, we wish the designed detector system to achieve the same statistical uncertainty in neutron counts when a pebble's burnup is more than 50,000 MWD/MTU. By this requirement and using the neutron emission rate of 13500 n/s/pebble at 80,000 MWD/MTU and the emission rate of 2670 n/s/pebble at 50,000 MWD/MTU, the minimal detection efficiency is given by

$$\eta_m = \frac{(1/0.05)^2}{30 \times 13500} \approx 1.0 \times 10^{-3} \text{ per source neutron}$$

while the target efficiency is determined as

$$\eta_t = \frac{(1/0.05)^2}{30 \times 2670} \approx 5.0 \times 10^{-3} \text{ per source neutron}.$$

With such efficiency, a detector system can measure a pebble's neutron emission accurately at least at high burnup levels.

## (2). Selection of candidate neutron detectors

Irradiated pebbles emit fast neutrons and numerous gammas. So the selected neutron detector should have not only high neutron detection efficiency but also good gamma discrimination ability (this issue will be discussed in detail in Sec. 4.3). Among the commonly used neutron detectors, gas detectors are suitable for serving both purposes. For example,  $\text{BF}_3$  tube usually has a high neutron detection efficiency due to the high thermal neutron cross-section of  $10-\text{B}(n, \alpha)$  reaction; in addition, the high Q value of this reaction assures  $\text{BF}_3$  tube to discriminate gammas effectively. Further more, photons have much less chance to interact with gas than with solid or liquid, so there would be only insignificant number of spurious pulses that are caused by direct interactions between photons and gas molecules in detector's sensitive volume. Similar statement is also applicable to He-3 proportional tube. Therefore, both types of detectors are suitable for this work. Fission chamber is also a candidate detector for this work because it has superior gamma discrimination ability due to its extremely high Q value. Other detectors based on scintillation processes are not suitable because of the enhanced gamma-ray sensitivity of solid or liquid scintillators and the radiation-induced spurious events that occur in photo multiplier tubes. Semiconductor detectors are very sensitive to radiation damage and are seldom used in reactor environments.

Table 4.2 Parameters of selected neutron detectors

Detector	$\text{BF}_3$ tube	Fission Counter	He-3 Counter
Diameter	5.08 cm	2.2 cm	5.08 cm
Length	38.1 cm	19 cm	38.1 cm
Detecting material	1 atm $\text{BF}_3$ gas, 96% of B-10	0.4 $\mu\text{m}$ Uranium coating, 90% of U-235	6 atm He-3 gas
Housing	Al, 1.5 mm	Al, 1.5 mm	Al, 1.5 mm

In summary,  $\text{BF}_3$  tube, He-3 proportional tube, and fission chamber were selected as candidate neutron detectors for the MPBR burnup monitor system. Although customized detectors can be constructed, it was

decided to use commercially available ones instead in this project. The physical parameters of these detectors are listed in Table 4.2.

### (3). MCNP simulations of detection efficiency and detector system design

For the selected neutron detectors, the detector-to-source responses were simulated by MCNP. In all the simulations, the following treatments or assumptions were made: (a). An irradiated pebble is used as the radiation source. Because the composition of a pebble during its lifetime does not change much and the composition does not affect neutron and gamma signals much, the initial composition of pebble is used in all the simulations. In addition, neutron source is assumed evenly distributed in the fuel kernel, with the neutron energy spectrum as that of Cm-244, since Cm-244 is the major neutron emitter; (b). The detector is put 20 cm away from the source; (c). Polyethylene is used as neutron moderator and is put either in front of the detector or around the detector, with the thickness of polyethylene being optimized to provide enough moderation for emitted neutrons; (d). To simplify the simulation, each reaction inside the detector sensitive volume is assumed to produce one neutron pulse and be counted. With this assumption, the simulated neutron count or efficiency is an ideal one. True detection efficiency of the same system should be lower than the simulated one because not all of the neutron pulses generated by nuclear reactions can be collected due to the gas multiplication effect, wall effect, space charge effect, and the use of a discrimination voltage for amplifier.

MCNP simulations were performed for the three selected types of detectors under different measurement setups. Results show that both  $\text{BF}_3$  tube and He-3 counter can have detection efficiency greater than  $1 \times 10^{-3}$  that barely meets the requirement; however, the detection efficiency of fission chamber is far below the requirement. Considering the assumption made in the simulations, we finally designed a multi-detector system to further improve the detection efficiency.

Figure 4.6 is a cross-sectional view of a three-detector system for He-3 and  $\text{BF}_3$  tubes. The bottom is a polyethylene plate with a gutter on which the pebble sits on. A 10 cm thick half lead tube is covered on the pebble as gamma shielding (see Sec. 4.3 for discussion of this). Next to the lead is a 10 cm thick half polyethylene tube with three detectors (either He-3 or  $\text{BF}_3$ ) embedded inside. The distance between the detector surface and the inner surface of the polyethylene tube is 1.6 cm. The lengths of detectors, lead tube and polyethylene tube are 38.1 cm. For such a three-detector system, detection efficiency was found to be as high as  $2.02 \times 10^{-2}$  and  $1.16 \times 10^{-2}$  for He-3 and  $\text{BF}_3$ , respectively, much better than the requirement.

In addition, a multi-fission-chamber detection system was designed that has 12 fission chambers embedded in a polyethylene half-cylinder, as shown in Fig. 4.7 (note that due to the high Q value of fission reaction, there is no need to use lead as gamma shield). The neutron response of this system was simulated by MCNP with two different thickness of Uranium coating (which we believe cover the normal range). The results are given in Table 4.3, which shows that even with the thin Uranium coating the system is still acceptable (of course, one can always increase the number of fission chambers to increase the detection efficiency) to reach the minimal requirement on detection efficiency for this on-line application.

Therefore, it is concluded that although low emission rate and short measurement time pose a challenge to neutron detection, it is feasible to design a system that can measure the neutron emission accurately within 30 seconds at high burnup levels.

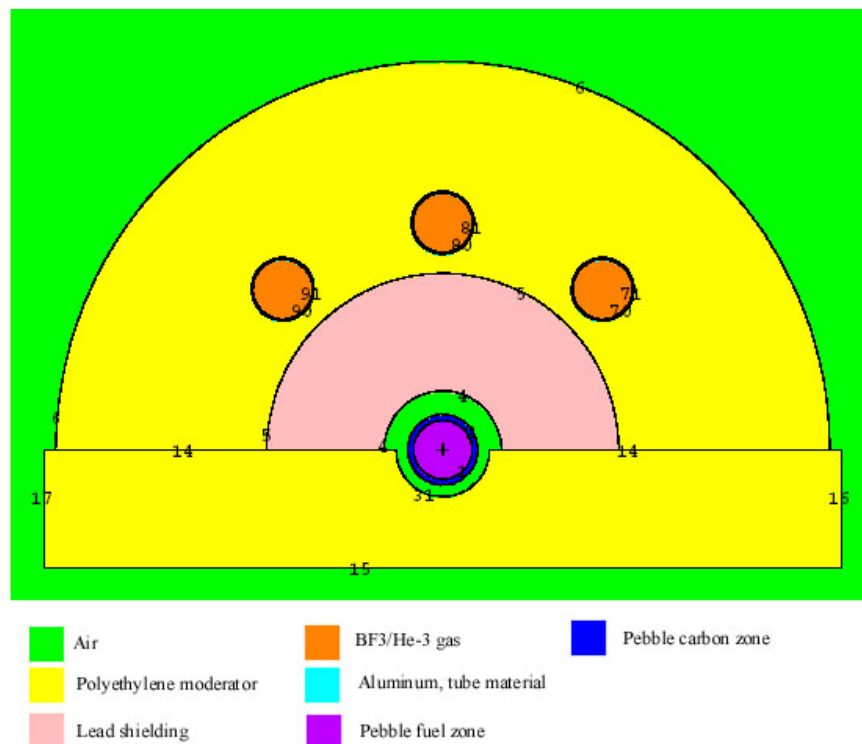
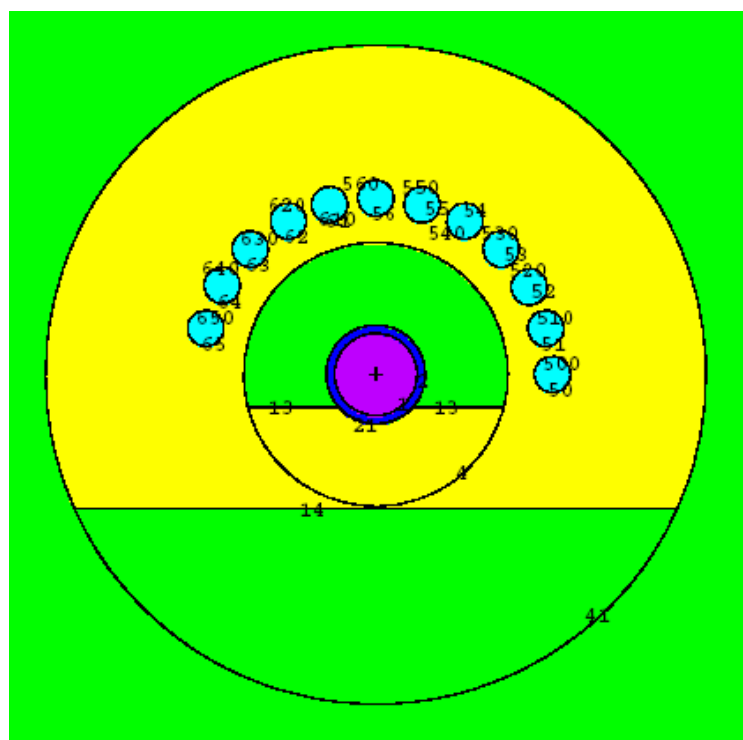
Figure 4.6 Sketch of a multiple He-3/BF<sub>3</sub> detection system.

Figure 4.7 Sketch of a multi-fission chamber detection system

Table 4.3. Simulated neutron response of the multi-fission chamber system

Configuration	Detection Efficiency
Fission chambers with 1.4 $\mu\text{m}$ Uranium (90%U-235) coating	$4.40 \times 10^{-3}$
Fission chambers with 0.4 $\mu\text{m}$ Uranium (90%U-235) coating	$1.28 \times 10^{-3}$

#### (4). Other studies on neutron detection

In addition to  $\text{BF}_3$ , He-3, and fission chamber, other neutron detection mechanisms were also investigated, including a conversion method that is based on  $(n, \gamma)$  reaction of Gadolinium, active neutron counting, active gamma counting, and the use SiC neutron detector. However, none of them was found suitable for the on-line burnup measurement due to either the low detection efficiency, or the incapability of discriminating gamma rays, or both.

### 4.3 Ability to discriminate gamma noises

The last issue in neutron measurement is to assess whether the designed neutron detector systems can discriminate gamma noises. ORIGEN2 outputs gamma emission in 18 groups (with energy ranging from 0.01MeV to 11.0 MeV) as a function of burnup. Most of emitted gammas have energies below 3 MeV. Total gamma emission rate increases with burn-up and its magnitude is in the order of  $10^{13}$  photons/sec/pebble. As shown in Fig. 4.8, irradiated pebbles emit much more (about 1 billion times more) gammas than neutrons. Those emitted gammas serve as strong background noises in neutron measurement. So it is very important for the designed neutron detector systems to discriminate such strong gamma noises in order to deliver credible neutron counts.

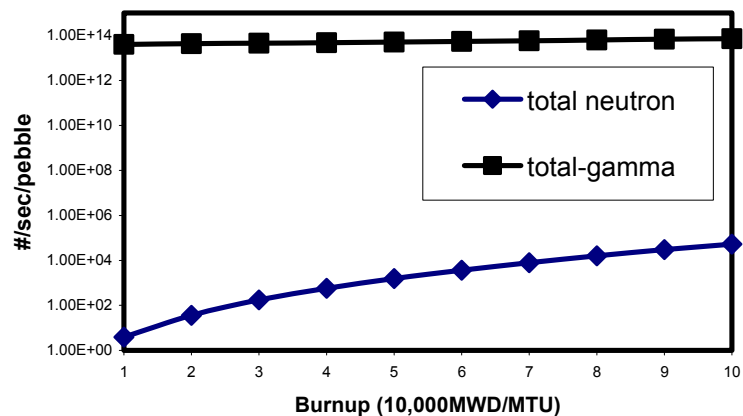


Figure 4.8 Comparison between gamma emission and neutron emission

#### (1). Gamma interference in the $\text{BF}_3$ and He-3 detector systems

By the physics of photon interactions, electric pulses produced by photons in gas neutron detectors have

much less energy than neutron pulses. By setting a proper energy bias in pulse counting, smaller pulses produced by photons can be easily blocked in low gamma fields. However, in strong gamma fields, both  $\text{BF}_3$  and He-3 tubes may lose neutron counting ability due to the effect of pulse pileup. As the increase of gamma dose rate, pulse pileup becomes more and more serious so that smaller photon pulses are summed up to form bigger ones in neutron detectors. Eventually these pulses may exceed the preamplifier's energy discriminator threshold and be counted as neutron events. It has been shown [5-8] that both  $\text{BF}_3$  and He-3 counters fail to work properly if gamma dose rate is too high. Specifically, a conventional  $\text{BF}_3$  tube can only successfully discriminate against gamma rays at exposure rates up to 12 R/h and a He-3 tube works well only at gamma exposure rate below 10 Rad/h. Therefore, gamma shielding is usually necessary in neutron measurement in strong gamma fields to achieve a better signal to noise ratio. As discussed in Sec. 4.2, lead was used as gamma shield in the MCNP simulations of the detection efficiency of  $\text{BF}_3$  and He-3 counters. Investigation was done to optimize the thickness of gamma shield and it was found that 10 cm lead is sufficient to reduce the gamma dose rates inside the  $\text{BF}_3$  and He-3 counters below the limits.

In addition to the limitations on gamma exposure rates,  $\text{BF}_3$  and He-3 counters also downgrade in performance after receiving a certain amount of gamma exposure. References [7-8] show that  $\text{BF}_3$  tubes start to fail after it receives a gamma dose of 23 R and He-3 tubes can stand for gamma exposure up to 2000 Rad. For the detector systems with 10 cm lead gamma shield, as sketched in Fig. 4.6, gamma dose rate in the  $\text{BF}_3$  and He-3 tubes was also simulated by MCNP. Results for gamma dose rates in the neutron detectors are given in Table 4.4, which shows that  $\text{BF}_3$  tubes can only continuously work 4.5 hours, measuring 541 pebbles, and He-3 tubes can continuously work 18.1 days, measuring 52,173 pebbles. Both types of the detector systems can only perform stably in a relatively short period of time. Thus, a single detector system is not enough for the on line continuous measurement. Two identical detection systems must be built and be used alternatively.

Table 4.4 Gamma Dose Rate in the Neutron Detectors

Detector	Gamma rate	Gamma Dose limit	Time of use
$\text{BF}_3$	5.10 R/h	23 R	4.5 hours
3-He	4.60 Rad/h	2000 Rad	18.1 days

## (2). Gamma interference in the multi-fission-chamber system

Gamma interference in the multi-fission-chamber system was also investigated. Gamma rays primarily interact with matter through photoelectric, pair production, and Compton scattering. These reactions can only generate pulses with energies less than the energies of the gamma rays involved in the reactions. Since the maximum energy of all gamma rays emitted from the pebble is no more than 10 MeV, all the pulses generated by such interactions of gamma rays can be easily eliminated because their energies are far below the pulse energies (greater than 50 MeV) produced by neutron fission reactions. Studies show that pulse pileup effect is not a serious problem for the multi-fission-chamber system

However, with small probability, high energy gamma rays can also have photonuclear reactions that emit neutrons or have photo-fission reactions in fission chambers. Analysis was done to demonstrate that the photonuclear and photo-fission reactions of high energy gammas have no effect on the neutron counting in fission chambers.

We first investigated whether such reactions of high energy gammas can cause extra neutron emission from

the pebble. Primarily, a fuel pebble contains Carbon, Oxygen, and Uranium. The gamma threshold energies for Carbon ( $\gamma, n$ ) and Oxygen ( $\gamma, n$ ) reactions are 18.72 MeV and 15.66 MeV, respectively. The thresholds for other photon-nuclear reactions that can also produce neutrons are even higher for Carbon and Oxygen. The photo-nuclear and photon-fission reaction of Uranium is about 5.26 MeV. Table 4.5 lists the emission rate of high energy gammas from a pebble at 80,000 MWD/MTU. It shows that no high energy gammas are emitted from activation products, limited number of gammas are emitted within 4-10 MeV from actinides, and a significant number of gammas are emitted only within 4-6 MeV from fission products. Additional analysis shows that the only significant fission product nuclide that can emit gammas within 4-6 MeV is Rb-88. Among the 30 discrete  $\gamma$  lines emitted by Rb-88, the highest one is 4.853 MeV, which is less than U ( $\gamma, n$ ) and U ( $\gamma, f$ ) reaction threshold energy. So practically, no gammas are emitted above 4.853 MeV from fission products and only gammas emitted from actinides have high enough energy to have photo-nuclear or photo-fission reactions with uranium in a pebble. However, the emission rate from actinides is low (in total 758 gammas per second within 4-10 MeV) and the corresponding cross sections for U ( $\gamma, n$ ) and U ( $\gamma, f$ ) reactions are low (much less than 1 barn). Hence, the neutron emission due to the U ( $\gamma, n$ ) and U ( $\gamma, f$ ) reactions, which was found to be much less than 1 neutron per second by detailed analysis, can be neglected.

We then examined the possibility that the high energy gammas emitted from actinides cause photo-fission reactions in the Uranium coating of fission chambers. It is easy to show that the number of fission reactions in fission chambers caused by such high energy gammas are negligible, compared to the number of fission reactions in fission chambers caused by spontaneous neutrons emitted from the pebble, because both of the gamma source strength and the cross section are significantly less than those of neutrons, as shown in Table 4.6.

Table 4.5 High-energy  $\gamma$  emission rate (#/s) from a pebble

<i>Energy Range</i>	<i>Activation products</i>	<i>Actinides</i>	<i>Fission Products</i>
4-6 MeV	0	672	$2.635 \times 10^6$
6-8 MeV	0	77	0
8-10 MeV	0	9	0
4-10 MeV, total	0	758	$2.635 \times 10^6$

Table 4.6 Comparison of emission rate and cross section for high energy photons and neutrons

	<i>Strength (#/sec)</i>	<i>Fission cross section (b)</i>
High energy gammas (4-10 MeV)	$7.58 \times 10^2$	0.2 (at 10 MeV)
Spontaneous neutrons	$1.35 \times 10^4$	582 (thermal)

Overall, we conclude that the neutron counts produced in fission chambers will not be interfered by gamma rays. Therefore, the multi-fission-chamber system can work properly for the on-line burnup measurement.

## 5. CONCLUSION

This project investigated the use of gamma spectrometry and passive neutron counting for on line fuel burn up measurement for MPBR. In terms of using gamma spectrometry, two possible approaches were identified for burnup assay. The first approach is based on the measurement of the absolute activity of Cs-137. However, due to spectral interference and the need for absolute calibration of the spectrometer, the uncertainty in burnup determination using this approach was found to range from  $\sim \pm 40\%$  at beginning of life to  $\sim \pm 10\%$  at the discharge burnup. An alternative approach is to use a relative burnup indicator. In this case, a self-calibration method was developed to obtain the spectrometer's relative efficiency curve based upon gamma lines emitted from  $^{140}\text{La}$ . It was demonstrated that the ratio of  $^{239}\text{Np}/^{132}\text{I}$  can be used in burnup measurement with an uncertainty of  $\sim \pm 3\%$  throughout the pebble's lifetime. In addition, by doping the fuel with  $^{60}\text{Co}$ , the use of the  $^{60}\text{Co}/^{134}\text{Cs}$  and  $^{239}\text{Np}/^{132}\text{I}$  ratios can simultaneously yield the enrichment and burnup of each pebble. A functional gamma-ray spectrometry measurement system was constructed and tested with light water reactor fuels. Experimental results were observed to be consistent with the predictions.

On using the passive neutron counting method for the on-line burnup measurement, it was found that neutron emission rate of an irradiated pebble is sensitive to its burnup history and the spectral-averaged one-group cross sections used in the depletion calculations, which consequently leads to large uncertainty in the correlation between neutron emission and burnup. At low burnup levels, the uncertainty in the neutron emission/burnup correlation is too high and neutron emission rate is too low so that it is impossible to determine a pebble's burnup by on-line neutron counting at low burnup levels. At high burnup levels, the uncertainty in the neutron emission rate becomes less but is still large in quantity. However, considering the super-linear feature of the correlation, the uncertainty in burnup determination was found to be  $\sim 7\%$  at the discharge burnup, which is acceptable. Therefore, total neutron emission rate of a pebble can be used as a burnup indicator to determine whether a pebble should be discharged or not. In terms of neutron detection, because an irradiated pebble is a weak neutron source and a much stronger gamma source, neutron detector system should have high neutron detection efficiency and strong gamma discrimination capability. Of all the commonly used neutron detectors, both the He-3 and  $\text{BF}_3$  detector systems were found to be able to satisfy the requirement on detection efficiency; but their gamma discrimination capability is only marginal. Even with thick gamma shielding, these two types of detectors shall deteriorate in performance after receiving certain amount of gamma exposure. Thus, two or more detector systems must be used alternatively for continuous measurement. On the other hand, fission chambers were found that they can effectively discriminate gamma interference for this on-line application even without using gamma shield. However, detection efficiency of fission chambers is low; thus a multi-fission-chamber system (using at least 12 commercially available fission chambers) must be used to achieve the required detection efficiency. Overall, passive neutron counting could be used to provide an on-line, go/no-go decision on fuel disposition on a pebble-by-pebble basis for MPBR, if the detection system is well designed.

## 6. REFERENCE

1. J.H. Gittus, "THE ESKOM pebble bed modular reactor," *Nucl. Energy*, Vol. **38**, pp. 215-221, 1999.
2. E. Russell, "A reactor for the emerging nations (pebble bed modular reactor)," *Int. Power Gen.*, vol. **22**, pp. 7-9, 1999.
3. A.C. Kadak et al., "Modular pebble bed reactor project – Annual report," MIT, Cambridge, MA, Tech. Rep. MIT-ANP-PR-075, 2000.
4. A. I. Hawari, R. F. Fleming, and M. A. Ludington, "High Accuracy Determination of the Realitive Full Energy Peak Efficiency Curve of a Coaxial HPGe Detector in the Energy Range 700-1300 keV," *Nucl. Inst. Meth. Phys. Res.*, vol. A398, pp. 276-286, 1997.
5. D.H. Beddingfield et al. *Nuclear Instrument and Methods in Physics Research A*, vol. 45, pp. 670-682, 2000.
6. L.V. East, R.B. Walton. *Nuclear Instrument and Methods*, vol. 72, pp. 161-166, 1969.
7. T. Tomoda, S. Fukakusa. *Nuclear Instrument and Methods in Physics Research*, vol. 224, pp. 557-565, 1984.
8. V. Kerghese et al. *Nuclear Instrument and Methods*, vol. 74, pp.355-357, 1969.

## APPENDIX

### PUBLICATION DEVELOPED UNDER THIS PROJECT

Two archival journal papers and a conference article have been published on this project:

- A.I. Hawari, J. Chen, B. Su, Z. Zhao, "Assessment of On-Line Burnup Monitoring of Pebble Bed Reactor Fuel Using Passive Gamma-Ray Spectrometry," *IEEE Transactions on Nuclear Science* **49**: 1249-1253, 2002.
- J. Chen, A.I. Hawari, Z. Zhao, B. Su, "Gamma-Ray Spectrometry Analysis of Pebble Bed Reactor Fuel Using Monte Carlo Simulations," *Nuclear Instruments and Methods in Physics Research A* **505** (1-2): 393-396, 2003.
- A.I. Hawari, B. Su, J. Chen, and Z. Zhao, "Investigation of On-Line Burnup Monitoring of Pebble Bed Reactor Fuel Using Gamma-Ray and Neutron Methods," *Transactions of American Nuclear Society* **85**: 98-99, 2001.

In addition, two other manuscripts are currently in preparation and will be submitted to journals to report more results obtained in this project.